INFORMATION TO USERS

This dissertation was produced from a microfilm copy of the original document. While the most advanced technological means to photograph and reproduce this document have been used, the quality is heavily dependent upon the quality of the original submitted.

The following explanation of techniques is provided to help you understand markings or patterns which may appear on this reproduction.

1. The sign or "target" for pages apparently lacking from the document photographed is "Missing Page(s)". If it was possible to obtain the missing page(s) or section, they are spliced into the film along with adjacent pages. This may have necessitated cutting thru an image and duplicating adjacent pages to insure you complete continuity.

2. When an image on the film is obliterated with a large round black mark, it is an indication that the photographer suspected that the copy may have moved during exposure and thus cause a blurred image. You will find a good image of the page in the adjacent frame.

3. When a map, drawing or chart, etc., was part of the material being photographed the photographer followed a definite method in "sectioning" the material. It is customary to begin photoing at the upper left hand corner of a large sheet and to continue photoing from left to right in equal sections with a small overlap. If necessary, sectioning is continued again — beginning below the first row and continuing on until complete.

4. The majority of users indicate that the textual content is of greatest value, however, a somewhat higher quality reproduction could be made from "photographs" if essential to the understanding of the dissertation. Silver prints of "photographs" may be ordered at additional charge by writing the Order Department, giving the catalog number, title, author and specific pages you wish reproduced.

University Microfilms

300 North Zeeb Road
Ann Arbor, Michigan 48106

A Xerox Education Company

SURFACE DIFFUSION AND ITS DEPENDENCE ON SURFACE WATER

by

Ralph Tzu-Bow Yang

A Dissertation

Presented to the Faculty

of the Graduate School of Yale University

in Candidacy for the Degree

of

Doctor of Philosophy

1971

ABSTRACT

A method of measuring surface diffusion coefficient has been developed which involves the application of internal reflection spectroscopy. Surface diffusion coefficients for the system stearic acid on (0001) α-alumina have been measured under various surface conditions.

Higashi's model of predicting the dependence of surface diffusion coefficient on surface coverage in the submonolayer region was modified. The modified model showed definite advantage over the original one in correlating the experimental data from various sources.

The effect of the surface coverage of one species on the surface diffusion coefficient of another species has been studied. The following model systems were chosen in this work: (1) stearic acid/water on (0001) surface of α-alumina, and (2) stearic acid/water on KRS-5 surface. The rate of surface diffusion was measured as a function of surface coverage of adsorbed water, θ. In system (1), the diffusion rate is small at $\theta = 0.4$, increased by over two orders of magnitude as θ approaches one and decreased rapidly as θ was increased beyond one. While in system (2), a rather weak dependence of the diffusion rate of stearic acid on the amount of adsorbed water was found.

In the study of adsorption from solution, Harkins' assumption about the amount and orientation of the adsorbed species was examined. This assumption was found to be invalid for the system germanium/stearic acid (from carbon tetrachloride). On the other hand, stearic acid molecules adsorbed from solution in carbon tetrachloride onto the surface of alumina showed some degree of orientation.

ACKNOWLEDGEMENTS

I am deeply indebted to my advisers, Professor John B. Fenn and Professor Gary L. Haller. Professor Fenn is a constant source for diffusion of wisdom and inspiration, and he taught me what patience is. Professor Haller introduced to me the fields of catalysis, spectroscopy and especially the techniques of internal reflection spectroscopy. Their kind understanding, helpful advice and guidance throughout this research are greatly appreciated.

I should like to express my gratitude to Professor Uri Navon, who, with Professor Fenn, guided the work on the structuring effect of interfaces on water.

I wish to thank Professor Daniel E. Rosner and Professor Philip A. Lyons for their interest and advice in this work.

Thanks are also due to Mr. Richard W. (Bud) Rice who provided the adsorption isotherms of water on alumina.

A Yale University Fellowship for the year 1967-1968 is appreciated.

The Office of Saline Water is gratefully acknowledged for Grant 14-01-0001-1833 which made the research possible.

TABLE OF CONTENTS

CHAPTER I

INTRODUCTION AND BACKGROUND

Among the many phenomena associated with interfaces, a most interesting one is the interaction between a gas and a solid surface. Although adsorption has been widely investigated for years, the behaviors and properties of the adsorbed molecules are understood only poorly. One interesting characteristic is their ability to migrate to other sites on the solid surface while still in the adsorbed state. This surface migration is of great importance and of increasing interest in catalysis, in gas flow through porous media, in metallurgy, in treatment of fibers, and even in the movement of water or petroleum through the earth's structures.

Surface diffusion has recently been studied by some, although not many, researchers. Due to the limited knowledge about the nature of the surface itself, and the experimental difficulties, the investigation of this phenomenon is still at a primitive stage.

Of interest for the present study is the rather limited amount of work which has been done concerning the effect of surface concentration on the rate of surface diffusion of <u>single</u> adsorbed species[1]. The most pronounced feature is the increase of diffusion rate as surface concentration increases in the sub-monolayer region. The prevalent concept now is that molecules detach from a site and hop about freely until they find another empty site[2]. According to present theories based on this concept, as surface coverage increases, the diffusion rate approaches infinity at monolayer coverage, i.e., when all sites are occupied.

Experimental data do not support this conclusion. An extension of these theories is presented in Chapter II, and a better agreement with the experimental data is shown.

A standard method of measuring surface diffusion coefficient has been followed by many workers[3]. It involves measuring the total mass flux across a porous media and splitting it into two parts, one due to gaseous diffusion and the other to surface diffusion. The gaseous diffusion rate is in principle calculable and can be subtrated from the total rate to give the surface rate. Complexity and uncertainties are involved in this splitting process[4]. It is the purpose of Chapter III to describe and to present some results from a much more direct method of measuring the rate of surface diffusion. This method is based on the application of internal reflection spectroscopy coupled with the approximate solution to the diffusion equation under pertinent boundary conditions.

Another method of measuring the rate of surface diffusion by direct counting of radio-active labelled materials was used by Rideal[28].

As has been mentioned, all former work on surface diffusion is limited to cases involving a single adsorbed species. Chapter IV deals with the surface diffusion of one species in the presence of another adsorbed species. In particular, measurements were made on the diffusion of stearic acid over surfaces on which water molecules were adsorbed. The two surfaces studied were single crystal α alumina and a poly-crystalline thallium halide known as KRS-5.

The direction of surface diffusion is that of decreasing surface concentration. If Fick's law is obeyed, the proportionality constant between surface mass flux and surface concentration gradient is called "surface diffusion coefficient".

Einstein's Brownian motion (or random walk) model of the diffusion process applies to surface diffusion as well as to bulk diffusion. It leads to the following expression for the diffusion coefficient:

$$D_s = \frac{d^2}{2\tau} \tag{1}$$

where D_s is surface diffusion coefficient, d is the distance between adjacent sites at which molecules can stick and τ is the holding time at such a site.

Hill[5] applied Eyring's absolute rate theory, assuming that surface diffusion is an activation process, and derived a relationship for the holding time τ.

$$\frac{1}{\tau} = \frac{kT}{h} \cdot \frac{F_s^*(T)q_x^*(T)q_z^*(T)Z}{F_s(T)q_x(T)q_y(T)q_z(T)} \cdot e^{-E/kT} \tag{2}$$

where F_s is the internal partition function of an adsorbed molecule on surface, q_i the partition function for vibration of an adsorbed molecule in the i direction, Z the number of nearest neighbor sites, h Plank's constant, and the asterisk denotes the value at the top of potential barrier E, or activated state.

In equation (2), the pre-exponential factor is the number of "attempts" to leave its site made by the molecule per second. The exponential factor is the probability that an attempt will be successful. Hence, τ is the actual holding time a molecule stays in a site. Approximations were made about the relative magnitudes of the partition functions in equation (2) so that the order of magnitudes of τ could be obtained. From equation (1), D_s could then be estimated.

Hill's model provides a reasonable physical picture of the surface diffusion process, but it is inadequate in explaining the effect of

surface coverage, θ, on D_s. It assumes that the adsorbed molecule can not jump to an occupied site. In such a case Z can be replaced by $Z(1 - \theta)$ and D_s becomes directly proportional to $(1 - \theta)$. This result is unfortunately exactly opposite to the experimental observation.

Higashi et al.[2] assumed that the activated molecule can jump to any site. If the site is empty, the molecule occupies it. If it is occupied, the molecule collides with the occupying molecule and scatters isotropically. The molecule continues to jump from site to site until it finds one empty. The average number of jumps is

$$n_\theta = \sum_{k=1}^{\infty} k(1 - \theta)\theta^{k-1} = \frac{1}{1 - \theta} \qquad (3)$$

Higashi postulates that $1/\tau$ in equation (1) should be replaced by n_θ/τ giving

$$D_s = \frac{d^2}{2(1 - \theta)\tau} \qquad (4)$$

By this relation D_s is inversely proportional to $(1 - \theta)$, in reasonable agreement with experimental data when θ is small relative to unity. It deviates from the experimental data as θ approaches one and goes to infinity at $\theta = 1$. Inspite of its shortcomings, this model is an advance in the theory of surface diffusion because it incorporates a "steric" factor which can speed up the rate of diffusion.

Carman[6] attributed the variation in D_s to surface heterogeneity. The sites with higher activation energy for diffusion are more readily occupied as θ is increased. The lower-energy sites with shorter residence times determine the diffusion rate, hence the increase in D_s.

Gilliland et al.[7] developed a model for surface diffusion based on

hydraulic theory. It pictures surface flow as occuring under the influence of a two-dimensional "spreading pressure". McIntosh[1] proved this model to be relatively unsuccessful in correlating his experimental data.

Perkingson[8] assumed that the activation energy for diffusion was proportional to the heat of adsorption. Based on this assumption, his experimental data for CO_2, SO_2, NH_3, and iso-C_4H_{10} flowing through porous Vycor glass were correlated. Moreover, D_s was found to be proportional to $\sqrt{T}$ empirically.

Hwang[9] assumed a model involving hindered translational motion of the activated molecules as opposed to the conventional models of free translational motion and no translational motion of the activated molecules. From this assumed model, Hwang found a working equation which is formally similar to Hill's.

Reyes[10] proposed that the frequency of jumps from the surface made by an adsorbed atom is determined by the energy exchange between the absorbed atom and the solid underneath. A one-dimensional model, i.e., the adsorbed atom is bound to the surface of a one-dimensional crystal, was used for the energy exchange process. The pre-exponential factor for the diffusion coefficient was calculated based on this model. It was compared with experimental data for several systems and showed reasonable agreement.

CHAPTER II

MODIFICATION OF HIGASHI'S MODEL

Higashi's model is in reasonable agreement with the experimental data for surface diffusion up to a$\theta$of about 0.6, this will be shown later in this chapter for several diffusion systems. At higher θ the theoretical values start getting greater than the experimental ones and go to infinity at $\theta = 1$. The interactions among the diffusing molecules can not account for this discrepancy, as the experimental curve would deviate even more from Higashi's model after taking the interactions into account[2]. Nor does it help to take into account the heterogeneity of surface sites, i.e., variation in activation energies. D_s would then be even greater toward $\theta = 1$ because the molecules tend to occupy higher energy sites at any given surface coverage. Moreover, an attempt by McIntosh[1] to incorporate the "flight time" in the analysis was not successful. Most previous investigators have concluded that flight time is a negligible contribution to the diffusion time, at least in the regime when $\theta < 1$.

Higashi assumed that a molecule would jump off instantaneously when hitting at an adsorbed molecule. This assumption suggests that the energy level of a molecule in the second layer is equal to the energy level at the top of the energy barrier for surface diffusion. Following this assumption, second layer adsorption could not take place before a full monolayer is completed. This is not true as multilayer adsorption does occur before surface coverage reaches unity, especially in the case of physical adsorption. This fact suggests that the energy level of the second layer can be lower than

that of activation energy for diffusion.

By allowing for the possibility of a finite holding time on an occupied site, i.e., "second layer" adsorption, we may write for the holding times,

$$\frac{1}{\tau_1} = \gamma_1 \cdot e^{-\Delta E_1/RT} \tag{5}$$

$$\frac{1}{\tau_2} = \gamma_2 \cdot e^{-\Delta E_2/RT} \tag{6}$$

where γ is the frequency of oscillation of the adsorbed molecule against the surface in the normal direction, and subscripts 1 and 2 denote first and second layers respectively. The relation between ΔE_1 and ΔE_2 is illustrated in the potential energy diagram as shown in Figure 1.

Now that the molecule makes $(n_\theta - 1)$ "stops" with holding time τ_2 at each stop before it occupies an empty site. Therefore, the average time τ for covering distance d in the random walk model should be replaced by τ_a, and τ_a is given by

$$\tau_a = \frac{\tau_1 + (n_\theta - 1)\tau_2}{n_\theta} \tag{7}$$

here $n_\theta = \frac{1}{1 - \theta}$ as calculated by Higashi[2]. Hence,

$$\tau_a = \tau_1\left(1 - \theta + \theta \cdot \frac{\gamma_1}{\gamma_2} e^{-(\Delta E_1 - \Delta E_2)/RT}\right) \tag{8}$$

If τ in the random walk model is replaced by τ_a from equation (8), the following expression is obtained:

$$D_{s,\theta} = \frac{d^2}{2\tau_1} \cdot \frac{1}{1 - \theta + \theta \cdot \frac{\gamma_1}{\gamma_2} e^{-(\Delta E_1 - \Delta E_2)/RT}} \qquad (9)$$

or

$$\frac{D_{s,\theta}}{D_{s,\theta=0}} = \frac{1}{1 - \theta + \theta \cdot \frac{\gamma_1}{\gamma_2} e^{-(\Delta E_1 - \Delta E_2)/RT}} \qquad (10)$$

The activation energies ΔE_1 and ΔE_2 can be evaluated experimentally. However, since the experimental data on heats of adsorption are more readily available, as well as being easier to measure, we may estimate the value of $\Delta E_1 - \Delta E_2$ by taking the difference in heats of adsorption between the first and second layers, as illustrated in Figure 1. This estimation assumes that the energy levels for diffusion are the same for both layers.

The quantity $\frac{\gamma_1}{\gamma_2}$, while difficult to evaluate experimentally, may be expected to be close to unity, and equation (10) becomes

$$\frac{D_{s,\theta}}{D_{s,\theta=0}} = \frac{1}{1 - \theta + \theta\, e^{-(\Delta E_1 - \Delta E_2)/RT}} \qquad (11)$$

This modification to Higashi's model gives a better fit to the experimental data from various sources and does not blow up at $\theta = 1$. That there is better agreement with experimental data is shown in Figures 2, 3 and 4.

Higashi's own experiments[2] on surface diffusion of propane on silica glass are shown in Figure 2. Equation (11) with $\Delta E_1 - \Delta E_2 = 1.58$ kcal/mole is plotted in this figure and shows satisfactory

agreement with the experimental data. Data for D_s at $\theta > 0.8$ for this system are not available.

Carman and Raal[6] calculated the activation energies for surface diffusion for the system CF_2Cl_2 - carbolac at various surface coverages, by the use of Arrhenius plots. The activation energy stays quite constant at 3.3 kcal/mole in the monolayer region, and constant at 2 kcal/mole between $\theta = 1.2$ and $\theta = 1.8$[6]. Such behavior indicates that $\Delta E_1 - \Delta E_2 \cong 1.3$ kcal/mole. By using this value, equation (11) was plotted in Figure 3. Again, a satisfactory agreement with the data of Carman and Raal is obtained.

Another deficiency of the original Higashi model is its indication that $D_s/D_{s,\theta=0}$ is independent of temperature. However, the experiments of Ross and Good[11] and of Carman and Raal[6] showed definite temperature dependence of $D_s/D_{s,\theta=0}$. This discrepancy is overcome by our modification as indicated in equation (10), which predicts a strong effect of temperature on $D_s/D_{s,\theta=0}$. It should be noted that γ_1/γ_2 also has a temperature dependence, although it is difficult to measure and the temperature dependence might be negligible at moderate temperature. The experimental data of Ross and Good for the system of n-butane - spheron 6 (2700°) carbon black at 30°C and 41.7°C are plotted in Figure 4. The heats of adsorption of this system were also measured as a function of θ, covering the range from $\theta = 0$ to 1.2. Heat of adsorption stays constant at about 8 kcal/mole in the monolayer region and drops to about 5.9 kcal/mole at $\theta = 1.2$. It would be a reasonable estimate that the difference between the heats of adsorption of the first and the second layers is 2.1 kcal/mole. Using this value as $(\Delta E_1 - \Delta E_2)$ in equation (11), provided a very good match with the

experimental data at 41.7°C. For the data at 30°C, equation (10) was used, with the same value for $(\Delta E_1 - \Delta E_2)$. A value of 1.5 for γ_1/γ_2 was required to fit the experimental data.

The validity of equations (10) and (11) thus seems to be supported by various experimental data. A final remark about these equations is the following. Based on the complex temperature dependence shown in equation (10), an Arrhenius plot of log D_s over $\frac{1}{T}$ would give a straight line only at $\theta = 0$. At higher coverages, a slightly bent curve should be obtained. It then becomes necessary to know the values of $(\Delta E_1 - \Delta E_2)$ and γ_1/γ_2 in order to obtain the exact value of activation energy for surface diffusion.

CHAPTER III

EXPERIMENTAL METHODS

As stated in Chapter I, two major methods of measuring the rates of surface diffusion of organic materials on solid surfaces were used by previous investigators. One involves the measurements of flow of gases through porous media. The other is by a direct counting of labelled materials.

In this work, the recently developed technique of internal reflection spectroscopy is applied to measure the rate of surface diffusion.

1. The IRS Method

The practical and theoretical aspects of internal reflection spectroscopy (IRS) have been well documented by Harrick[12]; therefore, only a very brief description of the technique is given here.

When a beam of light is incident on the interface of two media from the optically denser medium, there exists a critical angle which can be obtained from Snell's law. If the angle of incidence exceeds the critical angle, the incident beam is totally reflected. When there is no light-absorbing material present at the interface, there is no net energy flow into the rarer medium. However, there exists an electromagnetic field in the rarer medium whose electric field amplitude decays exponentially with distance from the interface[12]. The depth of penetration is defined as the distance required for the electric field amplitude to fall to 1/e of its value at the interface. This depth is in the order of the wavelength. When materials are present at the interface and are within the penetration depth,

some energy of the light beam is going to be absorbed. Thus, it is possible to obtain the absorption spectra of the deposited materials. This effect has been used to provide an attractive analytical tool, and the phenomenon is known as internal reflection spectroscopy.

Furthermore, the signal can be amplified by multiply reflecting the light beam through the prism, such a prism is called an internal reflection element (IRE). As the number of reflections can be made very large, a very minute quantity of material on the surface can be detected. The spectrum with strong absorption bands of a deposited stearate monomolecular film on the surface has been obtained[13].

2. Apparatus, materials and procedure

(a). Apparatus and materials

All infrared spectra were recorded on a Beckman IR 12 spectrophotometer in the double beam mode. The IRS cell and mirror set were manufactured by Wilks Scientific Corporation. The cell consisted of a stainless steel circular chamber with gas outlet and inlet, and two window ports on the side. The sapphire windows were blazed onto nickel flanges and sealed to the cell with Viton "O" rings. The IRE was clamped into a stainless steel block suspended from the lid which could be sealed to the main body of the chamber. Two heater wells with a thermocouple well between them were bored through the lid into the stainless steel block from outside the chamber. A model 1211 temperature controller manufactured by Pak-Tronics, Inc. was used to maintain a constant cell temperature within $0.1^{o}F$. The temperature controller probe and a fine iron-constantan thermocouple joint were placed into the center well which was very close to the IRE. The operating temperature was always within $20^{o}C$ of room temperature.

Temperature gradients within the cell were therefore small. The resulting uncertainties in the temperature of the IRE were thus negligible. This assertion is supported by the fact that even during other experiments at temperatures above 400°C the difference in temperature between the IRE and the thermocouple was less than 5°C.

The IRE for most experiments was an aluminum oxide prism. It was cut and polished from a flame fusion-grown single crystal by Adolf Meller Company. The dimensions were 52 x 20 x 0.5 - mm. The major face was cut parallel to the (0001) plane. The ends were beveled to 45° to form entrance and exit aperatures, and provided for about one hundred 45° internal reflections. The surface was polished with diamond dust to an average roughnesss of 100 Å (measured by Meller). The KRS-5 IRE used was synthetic mixed crystal with 42 mole % thallium bromide and 58 mole % thallium iodide manufactured by Wilks Scientific Corp. Its dimensions were 52 x 20 x 1 - mm, also with ends beveled to 45°. It provided about fifty 45° internal reflections. Stearic acid labelled 99% + pure was used as received from Nutritional Biochemicals Corp. All water used for washing, supporting monolayers and as a source of vapor was doubly ion-exchanged, passed through an organic removal filter, and then distilled. All other chemicals were of laboratory reagent grade.

(b). Procedure

Alumina IRE was cleaned with warm chromic acid and distilled water. Further treatment with concentrated nitric acid assured the removal of any chromium ions attached to the surface. The crystal was then flushed with distilled water and dried in an oven. After this treat-

ment, the absorbance of hydrocarbon left on the surface was less than 1% of the absorbance due to a deposited compressed stearate monolayer.

The KRS-5 IRE was cleaned with nearly boiling methyl ethyl ketone and chloroform. Under the best conditions with this cleaning method, hydrocarbon left on the surface corresponded to about 5% of a deposited stearate monolayer.

After cleaning the IRE crystal, stearic acid was deposited on the edges along the 52 - mm length as line sources for surface diffusion. Deposition of stearic acid was done by dipping the edges of the IRE into a concentrated solution of stearic acid in n-hexane. The volatile solvent was vaporized and a layer of bulk stearic acid was left on the surface. At the moment of dipping, the time was recorded as $t = 0$ for surface diffusion. After the IRE was in place, the chamber was filled with 99% + pure helium having a controlled water vapor content. By changing the water vapor content, the amount of absorbed water on the IRE surface was changed. The chamber was then sealed and IR spectra were recorded throughout the diffusion process over a period of about 20 hours. The peak intensity of the asymmetric stretching band of the methylene groups at $2928cm^{-1}$ was used as a measure of the amount of stearic acid present on the surface. The peak intensity of the water band at $3400cm^{-1}$ was used as a measure of the amount of adsorbed water. The spectra of C-H bands were normally amplified by 10 times by using the expanded scale of the spectrophotometer. Spectra were recorded at the intervals ranging from 15 minutes to several hours, being more frequently in the initial period. D_s was then calculated in the manner shown in the next section.

In the experiments for measuring diffusion rates from monolayers,

the monolayers were deposited from a Langmuir trough using Blodgett's technique[14]. For stearic acid monolayers the pH of the water in the trough was reduced to 4 by adding hydrochloric acid. For barium stearate monolayers the pH was adjusted to 8.5 by addition of dilute NaOH, the trough containing 9×10^{-4} M-$BaCl_2$ and 6.8×10^{-4} M-$NaHCO_3$. The optimum pH values used here were suggested by the previous workers[14,30]. Oleic acid was used as piston oil which exerted a surface pressure of 29.5 dynes/cm at 20°C. The deposited monolayer was then used as the source for diffusion. The same procedure for measuring the rate of diffusion from a bulk material was followed to measure the rate of diffusion from the deposited monolayer.

3. Determination of surface diffusion coefficient

The IRE was masked so that the infrared beam was blocked from the region in which the stearic acid was deposited. The recorded spectra related only to the materials which diffused on to that portion of the surface which was initially clean. As the diffusion occurred toward the originally bare portion of the IRE surface, the infrared absorption increased in direct proportion to the amount of material which had diffused out of the masked area.

Assuming that the diffusion from the deposited bulk stearic acid is equivalent to a two-dimensional diffusion process; obeying Fick's law, the diffusion equation is,

$$\frac{\partial C}{\partial t} = D_s \frac{\partial^2 C}{\partial x^2} \qquad (12)$$

where C is surface concentration, t the time, x the distance from the deposited material, and D_s the surface diffusion coefficient. C is a function of x and t only because stearic acid is deposited

on one side of the IRE uniformly so that there is no concentration gradient in the direction perpendicular to x.

The boundary conditions are

$$\begin{aligned} t = 0 &, \; C = 0 \\ x = 0 &, \; C = C_o \\ x = b &, \; \frac{\partial C}{\partial x} = 0 \end{aligned} \tag{13}$$

here x = b is at the edge of the IRE (b = 2 cm in our case).

C_o is the source "strength" for the diffusion process, or the effective concentration at x = 0, the source boundary. It is tempting to draw an analogy between C_o and the concentration of vapor in equilibrium with a liquid surface acting as a source for diffusion limited vaporization. In these terms C_o would be expected to have a strong temperature dependence. It should also be independent of the physical "structure" of the bulk material. Actually, we found that C_o had a very weak temperature dependence. For our present purpose we will simply note that C_o is the effective source strength, that it was temperature independent and that it remained constant throughout an experiment. We also assume in the absence of any information to the contrary that C_o does not depend upon the amount of water adsorbed on the surface. The bases for these assertions will emerge in the following discussions.

The solution of equations (12) and (13) is

$$C(x,t) = C_o \left[\operatorname{erfc} \frac{x-2b}{\sqrt{4D_s t}} + \operatorname{erfc} \frac{x-6b}{\sqrt{4D_s t}} + \operatorname{erfc} \frac{x-10b}{\sqrt{4D_s t}} + \cdots \right.$$

$$- \operatorname{erfc} \frac{x-4b}{\sqrt{4D_s t}} - \operatorname{erfc} \frac{x-8b}{\sqrt{4D_s t}} - \operatorname{erfc} \frac{x-12b}{\sqrt{4D_s t}} - \cdots$$

$$+ \operatorname{erfc} \frac{-x}{\sqrt{4D_s t}} + \operatorname{erfc} \frac{-(x+4b)}{\sqrt{4D_s t}} + \operatorname{erfc} \frac{-(x+8b)}{\sqrt{4D_s t}} + \cdots$$

$$\left. - \operatorname{erfc} \frac{-(x+2b)}{\sqrt{4D_s t}} - \operatorname{erfc} \frac{-(x+6b)}{\sqrt{4D_s t}} - \operatorname{erfc} \frac{-(x+10b)}{\sqrt{4D_s t}} - \cdots \right] \tag{14}$$

The detailed solution is given in Appendix 1.

For relatively small "excursions" of diffusing material, i.e., $x \leq b$, a good approximation of equation (14) is

$$C(x,t) = C_o \operatorname{erfc} \frac{x}{\sqrt{4D_s t}} \tag{15}$$

Equation (15) gives less than 1% error under our conditions: $t <$ several days; $D_s < 10^{-5}$ cm^2/sec; $0 \leq x \leq b$.

$$\text{Total amount diffused} = \int_o^b C(x,t)\,dx$$

$$= C_o \sqrt{4D_s t} \left[\frac{1}{\sqrt{\pi}} - \frac{1}{\sqrt{\pi}} e^{-b^2/4D_s t} + \frac{b}{\sqrt{4D_s t}} \operatorname{erfc} \frac{b}{\sqrt{4D_s t}} \right]$$

$$\cong 2C_o \sqrt{\frac{D_s t}{\pi}} \tag{16}$$

The neglection of the final two terms in the bracket causes significant error when D_s and t are both large. For example, when $D_s = 2.5 \times 10^{-5}$ cm^2/sec and t = 1 hr., the sum of these two terms accounts for 3 % of the total; when $D_s = 2.5 \times 10^{-5}$ cm^2/sec, t = 10 hrs, the sum accounts for 36% of the total; the sum is always a negative quantity in our case. However, the value of D_s is normally smaller than 2.5×10^{-5} cm^2/sec; when D_s is close to this value, the one-term approximation in equation (16) is good only for the initial period.

Equation (16) shows that a plot of total amount diffused against $\sqrt{t}$ will give a straight line with slope = $2C_o\sqrt{\frac{D_s}{\pi}}$. In order to determine D_s from this slope, C_o must be known. We therefore consider the determination of C_o.

Determination of C_o

If a Langmuir-Blodgett monolayer of stearic acid is deposited on half of the IRE surface as the source for diffusing, the boundary conditions for equation (12) become

$$\begin{aligned} t = 0 &, \quad C = 0 \\ x = 0 &, \quad C = C_m/2 \\ x = b/2 &, \quad \frac{\partial C}{\partial x} = 0 \end{aligned} \tag{17}$$

where x = 0 corresponds to the center line which divides the monolayer covered region from the bare surface at t = 0, x = b/2 is at the edge of the bare side. C_m is the surface concentration of the deposited monolayer and is known from the deposition conditions, i.e., the surface area corresponding to the surface pressure exerted by the piston oil[14]. The fact that C at x = 0 is

only half of C_m stems from the fact that the monolayer source is not an infinite reservoir. This boundary condition is illustrated by the following pictures:

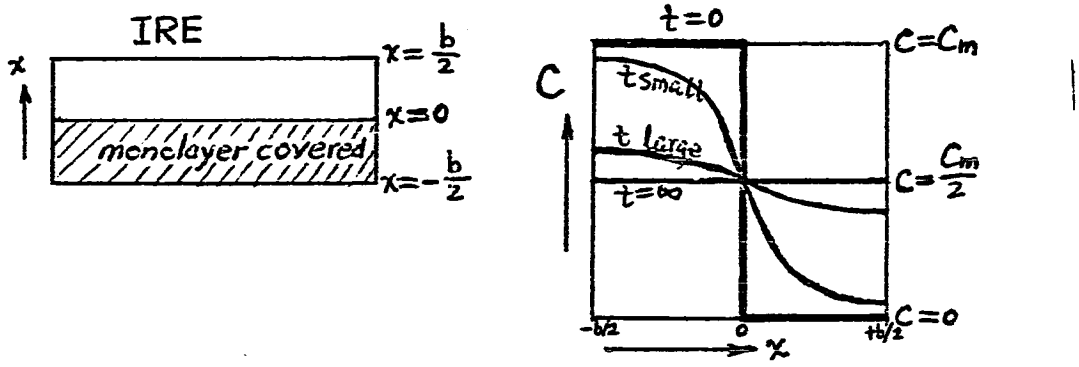

Another possible set of boundary conditions stem from the concept of "moving front". These boundary conditions state that $C \equiv C_m$ at the withdrawing front. They are not used here because of the obvious deficiency that there is always a discontinuity in concentration at the moving front.

The solution for equations (12) and (17) is of the same form as equation (14) and the approximated solution is

$$C(x,t) \cong \frac{C_m}{2} \operatorname{erfc} \frac{x}{\sqrt{4D_s t}} \tag{18}$$

Similarly,

$$\text{total amount diffused} \cong C_m \sqrt{D_s t/\pi} \tag{19}$$

By comparing equations (16) and (19) when D_s is the same for both cases, C_o can be obtained if C_m is known. It will be seen in the next chapter that in fact it becomes possible to determine D_s from the monolayer experiments without any knowledge of the actual value of C_m. In turn, a value for C_o can then be derived from

comparing experiments in which all the conditions except the nature of the source are identical.

4. Determination of the amount of adsorbed water

The fact that the absorption bands of water and of C-H are clearly resolved in the infrared region enabled us to measure the surface diffusion coefficient at various amounts of adsorbed water on the surface.

The adsorption isotherm of water on (0001) α Al_2O_3 was determined in terms of absorbance of the water band versus partial pressure of water vapor relative to the saturation value. The monolayer coverage of water was determined by BET analysis of the data. The amount of adsorbed water on the IRE surface in any particular diffusion experiment was then calculated by comparing the absorbance of the water band with that corresponding to a monolayer.

CHAPTER IV

RESULTS AND DISCUSSIONS OF RESULTS

1. Measurements of surface diffusion coefficients

As shown in equations (16) and (19), a plot of total amount of material diffused out of the deposited area against square root of time yields a straight line whose slope is proportional to the square root of D_s. For stearic acid monolayers, although the extinction coefficient of the methylene group varies from one group to another within each molecule[15], i.e., the methylene groups near the carboxylic group are more perturbed, it is assumed that the total extinction coefficient for each molecule is constant over the IRE surface. The total amount of stearic acid on the surface is therefore measured as the total absorbance of the infrared radiation by methylene groups. As long as the infrared beam is not incident on the source area, the change in absorption with time is due entirely to the material diffused out of the source area.

Figure (9) typifies the spectra recorded. It shows the growth of the C-H bands as a result of diffusion from a bulk stearic acid source on (0001) α Al_2O_3 at $40^{\circ}C$. The amount of water adsorbed on the surface in this experiment was 0.0952 in terms of adsorbance at 3400 cm^{-1}.

Figures (5) and (6) are the typical plots made to calculate D_s from the recorded spectra. The absorbance at 2928 cm^{-1}, which is the peak of the absorption band due to C-H anti-symmetric stretching of the CH_2 (or methylene) groups, is plotted against $\sqrt{t}$. Note that absorbance defined by the negative of natural logarithm of the

transmittance is used throughout the discussion.

Figure (6) shows results of an experiment in which a monolayer of stearic acid was deposited on half of the IRE surface as the source. Diffusion took place at 25°C. The ordinate shows total amount diffused as a fraction of deposited monolayer. The solution of the diffusion equation is, from equation (19),

$$\text{Fraction of monolayer diffused out} = \frac{\text{total amount diffused out}}{\text{total amount of deposited source}}$$

$$\simeq \frac{C_m \sqrt{D_s t/\pi}}{C_m \cdot b/2} = \sqrt{D_s/\pi} \cdot \sqrt{t} \qquad (20)$$

where $b/2 = 1$ cm in our experiments.

From the slope of the straight line in Figure (5), D_s was calculated by use of equation (20). The trouble with this measurement is the nuisance of depositing a monolayer by the rather intricate Langmuir-Blodgett technique. To simplify the experimental procedures, as the source bulk stearic acid was deposited from its hexane solution on the edges of the diffusion surface. Figure (6) is a typical plot of the results of the experiments of this kind. Again, D_s was calculated from the slope of the straight line, by use of equation (16). However, the slope is equal to $2C_o\sqrt{D_s/\pi}$, where C_o, the boundary concentration, is unknown. We therefore must determine the values of C_o.

C_o was calculated by comparing Figures (5) and (6), assuming the same D_s for both cases since both were under the same experimental conditions. It was found to be equal to an absorbance of 0.0691 per centimeter at 25°C, or 0.1382 over the total IRE surface which was 2 cm wide. To compare this value with the absorbance of 0.92 due to

an oriented monolayer[13], a correction must be made for the value of Co because the molecules are not compressed and are morelikely to be randomly oriented. For an oriented monolayer all the C-H bonds are parallel to the IRE surface. The correction factor due to the orientation is: A(C-H parallel to surface)/A(C-H randomly oriented) = $\frac{Ex^2 + Ey^2}{2} \Big/ \frac{Ex^2 + Ey^2 + Ez^2}{3}$ = 1.25, where A is the absorbance, Ex and Ey are the electric field amplitudes parallel to the IRE surface, Ez is that normal to the IRE surface. The values of the E's under the same experimental conditions are given in the paper by Haller and Rice[13]. After correcting for the orientation, C_o was found to be 1/5.35 of a compressed monolayer.

Figure (7) is the plot of fraction of stearic acid diffused out of a monolayer source against $\sqrt{t}$ at 40°C. Applying equation (20), D_s was calculated to be 7.82×10^{-6} cm^2/sec. The amount of adsorbed water was 0.062 in terms of absorbance at the peak of water band. By comparing with the results using bulk material as the source, in section 3 of this chapter, C_o was calculated to be 9% smaller than that at 25°C. While the opposite trend was expected, in view of the possible scattering of the data as discussed in section 3, we may well conclude that C_o stays roughly constant from 25°C to 40°C.

As mentioned in the preceding chapter, use of the one-term approximation in equation (16) may involve a significant error when D_s and t are large. In such cases, a plot of the total amount diffused against $\sqrt{t}$ will yield a curve which deviates more and more from the straight line as $\sqrt{t}$ increases. This behavior is shown in Figure (8), which is plotted from the spectra in Figure (9). In

Figure (8), the measured amount of the material diffused is less than that predicted by the straight line by about 40% at $\sqrt{t} = 3\ hr^{1/2}$. This discrepancy is due to the neglect of the last two terms in equation (16).

Clearly in this case only the initial part of the curve should be used in determining D_s. Therefore, whenever $D_s \geq 10^{-5}\ cm^2/sec$, the initial region around t = 1 hr was used to calculate D_s by the approximation in equation (16). The error in D_s by this precaution should be reduced to the order of only a few percent.

A question may be raised here as to whether the molecules diffuse individually or as clusters. It seems to have been generally accepted that surface diffusion involves only the random walk of single molecules. However, Bassett[16] observed rotation and translation of whole islands in his studies of the deposition of copper and silver on both amorphous carbon and graphite, and of silver on molybdenite, all at about 250°C. Reiss[17] calculated the potential energy surface for an island "adsorbed" on a crystal surface and explained the possibilities and conditions for the island to rotate and translate as a whole. According to this model, there are two ways for an island to move. Firstly, the island (which is assumed to be crystalline) must be "misoriented" with respect to the substrate. In other words, the lattices are mismatched energetically. Activation energy for moving as a whole decreases as the misorientation is increased. Secondly, the island may stay at a minimum potential energy and move when the island is growing in size, because the potential energy is also a function of its size.

For the case of the diffusion of stearic acid on alumina from

a bulk source, the source concentration is small, about 1/5 of compressed monolayer. Consequently, the concentration in the "dispersed phase" is extremely low. In our work it was usually less than 10 percent of a monolayer. Therefore, even after most of the diffusion had occurred, the formation of agglomerated stearic acid from diffusing molecules seems unlikely to have occurred. Furthermore, the source material was deposited on the surface from a solution. Consequently, the molecules would remain relatively mobile until the last traces of the solvent vaporized. Thus, mismatching of the lattices of the substrate and the deposited material, even if the latter does form a crystal, would be unlikely to happen. The second condition requires the growth of the islands as in the process of growing thin films. It does not seem to be applicable to our case. In other words, the process discussed by Reiss was equivalent in an overall sense to a "condensation". The process we consider is more nearly an evaporation, i.e., transfer from condensed to dispersed phases. For molecules which do not form a crystal and match well with the substrate lattice, the potential energy is zero according to Reiss's potential surfaces[17], and hence will not move as islands.

Another question may be asked about the mechanism of the diffusion process, that whether the observed "diffusion" might be due to the readsorption of the molecules which have been desorbed into the gas phase from the source area. If the surface diffusion process is a desorbed-gaseous-readsorbed process, changing the mean free path on the diffusing species in the gas phase would change the surface diffusion rate. However, surface diffusion rates measured with either

helium or air as the atmospheric gas at the same temperature and total pressure showed identical values. Thus, we conclude that in surface diffusion the molecules never get totally desorbed or out of the surface force region.

2. Measurement of surface coverage by water

In a quantitative study of the dependence of the surface diffusion rate of stearic acid upon the amount of water adsorbed on the surface, the measurement of the amount of adsorbed water is crucial.

We have adapted the BET formalism[18] and expressed the amount of surface water in terms of fractions or multiples of a monolayer. The symbol θ is used to represent this surface coverage. When θ is less than one, it represents the fraction of a monolayer. When it is greater than one there is more than a monolayer. Clearly, therefore, we must determine the absorbance corresponding to a monolayer, i.e., when $\theta = 1$. We will now consider this problem.

In considering the amount of water on an alumina surface we must recognize two kinds of surface species. Some molecules are relatively weakly bound and are considered physically adsorbed. The others are much more strongly bound and are generally referred to as chemisorbed. A further complication is that there seem to be two kinds of chemisorbed water. One adsorbs very quickly, the other very slowly. All of our surface diffusion experiments lasted for several hours. And the IRE was in contact with a humid atmosphere and also with liquid water (during the cleaning process) both for a long period of time before the diffusion experiments. Consequently, the slowly chemisorbed species was always present and contributed to the absorbance measurements which we used to determine the amount

of water on the surface. Therefore, we had to be sure that the surface was always saturated with respect to the slowly adsorbed species. On the other hand, the adsorption isotherm shown in Figure (10) was determined in a relatively short time so that the slowly chemisorbed component was not present. If we had waited long enough the isotherm would have been translated upward by an amount corresponding to the saturation by slowly adsorbed species. In fact, the absorbance corresponding approximately to the ordinate value of the plateau on the translated curve is what we define as the absorbance equivalent to a monolayer, i.e., $\theta = 1$. It includes contributions from both kinds of chemisorbed water as well as a physically adsorbed water in the BET sense. We will refer to this amount of absorbance as A_1. The reference level A_o at which the absorbance is zero refers to the condition of the surface after baking at 500°C and at a pressure of 10^{-5} torr for ten hours. This treatment removes all of the physically adsorbed water and essentially all of the chemisorbed water. Thus, by definition $\theta = A/A_1$ where A corresponds to the measured absorbance for a particular surface condition. In these terms, of course, when θ equals unity the surface is saturated with respect to chemisorbed water as well as with respect to the physically adsorbed water.

In actual practice we did not determine A_1 by waiting a long time in the isotherm determination. Instead, we determined the amount of adsorbance due to a physically adsorbed monolayer in a "rapid" isotherm experiment and added it to the background level of absorbance which remained after pumping for four hours at 30°C and a pressure of 10^{-5} torr, after having soaked the surface in liquid water for several hours. The actual value of the absorbance

after this treatment was 0.055. The additional absorbance due to a BET monolayer was 0.0363. Thus, $A_1 = 0.055 + 0.0363 = 0.0913$. More details about this analysis and the related experiments are given below.

The adsorption isotherm shown in Figure (10) was taken at 40°C, the temperature at which subsequent diffusion experiments were performed. This isotherm belongs to Type II according to the BDDT classification[19]. In order to make a BET analysis of the isotherm from Figure (10), the absorbance due to the chemisorbed species must be excluded. In Figure (10), all the absorbances were calculated based on a background spectrum of the crystal which was measured after several hours of evacuation at 500°C. This background reference level includes any absorbance due to traces of chemisorbed water which we referred to as A_o. It should be noted that it is relative to this background that all the calculations of surface coverage of water are made. Water vapor was then introduced and after several minutes of equilibration, the adsorption isotherm was taken in the direction of decreasing vapor pressure. When the vapor pressure was decreased to 10^{-5} torr, some water remained which was believed to be strongly chemisorbed. This residual amount of water was adsorbed quickly, but it required several hours to remove it at 500°C and 10^{-5} torr[13].

BET analysis was made without including this amount of chemisorbed water (Figure 11). A monolayer capacity of 0.0363 in terms of absorbance at 3400 cm^{-1} was obtained from this analysis.

To measure the amount of the chemisorbed water, the IRE was soaked in water for several hours at room temperature. It was followed

by pumping off at 10^{-5} torr for 4 hours at 30°C. The amount of water remained on the surface was of chemisorbed and had an absorbance of 0.055. Thus, we obtained the value of 0.0913 as the monolayer capacity.

It is interesting to compare the above calculated monolayer capacity with the data in literature in connection with the energetic considerations. The heat of adsorption of water on α alumina which had predominantly (0001) surface was found by Yao[21] to be about 30 kcal/mole for the first 20% of a monolayer. It decreased gradually to 20 kcal/mole for the next 40% of a monolayer, and remained fairly constant at 20 kcal/mole for the last 40% of a monolayer. The last regime is relatively physically adsorbed and corresponds to the regime in which the BET analysis in this work was made. The rest represents the chemisorbed water.

It is also interesting to compare this empirical value of monolayer capacity, i.e., 0.0913, with the one calculated for a close-packed layer of bulk water molecules. For a close-packed layer of water molecules, we assume that the O-O distance is 3 Å, and the thickness of the layer is also 3 Å. The extinction coefficient at the peak of absorption band of bulk water is available in literature[31]. Frech[31a] reported an extinction coefficient of 103 ± 4 liter $mole^{-1}$ cm^{-1} (base 10 logarithm in Beer's law) at the peak of the OH stretching band at 3387 ± 20 cm^{-1}, and at a temperature of 26°C. Using the above data, if the light beam passes normally through the layer of water molecules 100 times, which is the number of reflections in our experiments, the total absorbance (e-based logarithm) is 0.0416. In order to make a comparison between this value and our value for

monolayer capacity, it should be recalled that our value is related to the molecules adsorbed on the IRE surface. Therefore, we should consider a close-packed layer of water molecules sticking on an IRE surface. In this case, the thickness of the layer must be corrected for the interaction between the evanescent electric field and the thin layer of water[12b]. The strength of interaction can be conveniently expressed in terms of an "effective thickness". The effective thickness for the 3 Å - thick layer of water was calculated to be approximately 9.9 Å [12b]. Using the extinction coefficient reported by Frech[31a], the total absorbance is 0.137. This is the expected absorbance for a close-packed monolayer placed on the IRE surface if the water molecules retain the intermolecular bonding of bulk water and do not interact strongly with the surface.

In comparing our value of monolayer capacity, i.e., 0.0913, with 0.137 as calculated above, we consider two possible situations:

Case (1). If the extinction coefficient of adsorbed water molecules is slightly smaller than that of the bulk, both the chemisorbed and physically adsorbed water molecules are indeed <u>in the first layer</u>. In other words, the physically adsorbed water molecules do not form a second layer which sits on top of the chemisorbed water. The value of 0.0913 is indeed the monolayer capacity. Furthermore, $\theta = 2$ would correspond to the absorbance of about twice of 0.0913 or slightly larger, if the extinction coefficient of the second layer approaches that of the bulk.

Case (2). Now we consider a highly idealized model of the dry (0001) surface of α alumina, as shown in the following picture:

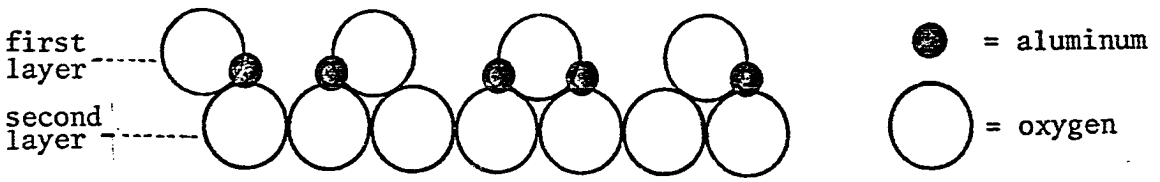

The 0-0 distance in an oxygen-saturated layer is roughly 2.8 Å[32]. It is a possibility that the so-called "chemisorbed water", which corresponds to the absorbance of 0.055, is the water filled in the cages in the top layer of the dry surface, and the picture becomes

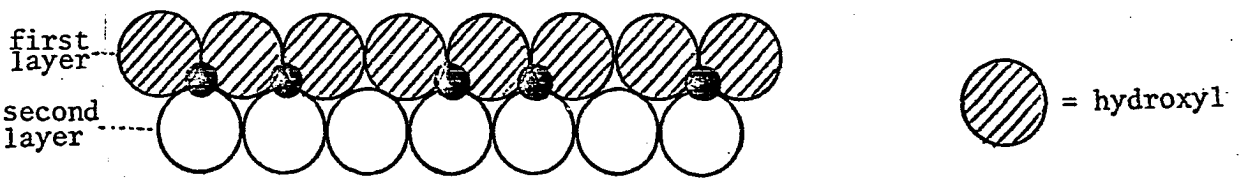

Consequently, the so-called "physically adsorbed water", which corresponds to the absorbance of 0.0363, is the water in the second layer (first physically adsorbed layer). In this case, the extinction coefficient of the "chemisorbed water" would be about $\frac{0.055 \times 2}{0.137} \simeq 0.8$ of that of the bulk, while the extinction coefficient of the physically adsorbed $\frac{0.0363}{0.137} \simeq 0.26$ of bulk extinction coefficient. Now that we have defined $\theta = 1$ at the absorbance of 0.0913, the absorbance for $\theta = 2$ would be about 1.3 if the second physically adsorbed layer has about the same extinction coefficient as the first physically adsorbed layer.

Case (1) appears more reasonable, since it does not require as

large a change in extinction coefficient compared to bulk water as case (2). In the discussion which follows, we will assume that the first layer of adsorbed water is complete ($\theta = 1$) when the absorbance equals 0.0913 and the second layer is complete ($\theta = 2$) at about twice this value.

3. The effect of surface wetness on D_s

A. Stearic acid diffusion on (0001) α Al_2O_3 at various surface wetnesses.

By adusting the partial pressure of water vapor in the atmosperic gas, (helium in this case), the amount of adsorbed water was controlled. The diffusion coefficient of stearic acid on (0001) surface of α alumina as a function of the amount of adsorbed water was measured and is shown in Figure (12). The temperatures for all the measurements fell in the range of 38.4°C to 40°C. The abscissa represents the amount of water on the surface in terms of absorbance at 3400 cm^{-1}. The ordinate is the logarithm of the diffusion coefficient D_s in cm^2/sec. The amount of adsorbed water was varied from about 4/10 of a monolayer to about two monolayers. It is to be remembered that water is largely physically adsorbed in this range.

All of the diffusion coefficients were calculated from the plots of total absorbance of diffused material against $\sqrt{t}$, as discussed previously. In Table I the experimental results are summarized.

TABLE I

Values of D_s for the system stearic acid - (0001) α Al_2O_3 at various surface wetness at 40°C.

Absorbance at 3400 cm^{-1}	θ	D_s cm^2/sec
0.0375	0.411	2.41×10^{-7}
0.04	0.438	2.13×10^{-7}
0.0625	0.685	6.55×10^{-6}
0.0766	0.839	1.683×10^{-5}
0.095	1.041	4.103×10^{-5}
0.0952	1.043	3.21×10^{-5}
0.1173	1.285	8.11×10^{-6}
0.135	1.479	9.48×10^{-7}
0.145	1.588	2.733×10^{-7}
0.163	1.785	≈ 0
0.1713	1.876	≈ 0

The strong dependence of the diffusion rate upon the amount of water adsorbed on the surface is clearly shown by the plot of these data in Figure (12). The diffusion rate goes up drastically from $\theta = 0.4$ to $\theta = 1.0$ and decreases as θ is further increased. This behavior suggest that there might be two competing mechanisms. One is dominating in the submonolayer regime. The other becomes dominant when θ is above unity.

In accordance with the ideas in previous theoretical treatments

discussed earlier, we consider in the submonolayer regime, the flying time of a diffusing stearic acid molecule is negligible as compared to the site-holding time. The activation of stearic acid is thus the rate-controlling process. However, when θ is greater than unity, there are many more activated (desorbed but still in the surface force field) water molecules over the surface than stearic acid molecules. This is due to the comparatively low activation energy of water. Therefore, a diffusing stearic acid molecule would experience numerous collisions with water molecules. The net result is that it would engage in a random walk with ever decreasing mean free path as θ increases. This two-dimensional hindered "Brownian movement" greatly lengthens the flight of an activated stearic acid molecule. Therefore, the flying time must be included in any attempt to calculate the diffusion rate in the beyond-monolayer-water-coverage regime.

With the above mechanisms in mind, the experimental results shown in Figure (12) are interpreted separately for these two regimes.

Sub-monolayer water coverage

(a) Modified Higashi's model

In the sub-monolayer region, the modified Higashi model in Chapter II is used to interpret the increasing feature of D_s as θ increases. According to equation (11);

$$\frac{D_s}{D_{s,\theta=0}} = \frac{1}{1 - \theta + \theta \cdot e^{-(\Delta E_1 - \Delta E_2)/RT}} \qquad (11)$$

here ΔE_1 refers to activation energy for release of a stearic acid molecule from an unoccupied alumina surface site, ΔE_2 refers to the

bonding between stearic acid and an adsorbed water molecule. A very crude approximation was made that $\Delta E_1 - \Delta E_2 = 1.22$ kcal/mole. There is no information in literature about the value of this quantity, but the assumed rather small difference between ΔE_1 and ΔE_2 could be understood viewing the fact that the heats of adsorption of n-fatty acids at the silica/benzene and silica/hexane interfaces are independent of surface coverage, as observed by Armistead et al.[22]. Using this value in equation (11), D_s has a seven-fold increase when θ is increased from 0.4 to 1, as shown in Figure (13). This increase is by far too small to explain the experimental data, which has three orders of magnitude increase over the same range of θ.

However, we have thus far considered only energetically homogeneous surfaces, with identical adsorption sites. On such sites heats of adsorption and also values of D_s would be independent of surface coverage of water. We will now consider the implications of surface heterogeneity, i.e., variation in heats of adsorption from site to site.

(b) Surface heterogeneity

By measuring heats of adsorption as a function of θ, Yao[21] has found strong surface heterogeneity on the same kind of surface as used in this study. This heterogeneity is also supported by the existence of different types of adsorption of water which we described in the preceding section.

Figure (14) is reproduced from the results by Yao[21]. It shows the variation of heat of adsorption of water with coverage on α alumina for which the predominant surface was (0001). A reasonable view is that the heat of adsorption of stearic acid would have about

the same variation. In other words, the degree of heterogeneity is the same for both cases, because the same type of polar groups are bound to the surface in each case.

At surface coverage θ, the fraction of the sites which are not covered by water is $1 - \theta$. It is the diffusion of stearic acid taking place on these sites which is rate-controlling. Furthermore, all these sites are energetically different according to the continually decreasing heat of adsorption with respect to θ. As θ goes up, more higher-energetical sites are occupied by water, and diffusion of stearic acid takes place on the lower-energetical sites which are unoccupied. Consequently, lower activation energies are required and the overall rate of diffusion is increased.

In order to account for the rate increase due to surface heterogeneity, an "average" activation energy $(\Delta E_\theta)_{avg.}$ may be defined such that,

$$D_{s,\theta} = D_{s,\theta=0.4} \cdot e^{-(\Delta E_\theta - \Delta E_{0.4})_{avg.}/RT} \tag{21}$$

$\theta = 0.4$ is used as reference since the experimental results start from this point.

Calculation of $(\Delta E_\theta)_{avg.}$ is based on the averaging of $D_{s,\theta}$ and obeys the following equations:

$$D_{s,\theta} = \int_\theta^1 D_s(\theta') \cdot f(\theta')d\theta' \tag{22a}$$

$$D_s(\theta') = k \cdot e^{-\Delta E_{\theta'}/RT} \tag{22b}$$

$$D_{s,\theta} = k \cdot e^{-(\Delta E_\theta)_{avg.}/RT} \tag{22c}$$

where $f(\theta')$ is a distribution frunction and k is a constant.

However, $(\Delta E_\theta)_{avg.}$ can not easily be calculated because the true value of activation energy for stearic acid diffusion as a function of θ is not known even though the heat of adsorption for water is known as a function of θ. Therefore, it is not intended here to attempt to calculate $(\Delta E_\theta)_{avg.}$ Rather, a curve of $(\Delta E_\theta - \Delta E_{0.4})_{avg.}$ as a function of θ which can account for the deviation of the experimental data from the modified Higashi model is shown in Figure (14). This empirical curve is similar to an arithmetic mean of $(\Delta H_\theta - \Delta H_{0.4})$, here ΔH is the heat of adsorption of water. The increase in diffusion rate due to the empirical $(\Delta E_\theta - \Delta E_{0.4})_{avg.}$ is shown in Figure (15). In Figure (13), a satisfactory match is seen between the experimental results and the preceding semi-theoretical arguments.

It is not appropriate here to consider more refined theories. We simply wanted to show that the modified Higashi model, which is for an idealized homogeneous surface, plus consideration of surface heterogeneity, can in principle account for the sharp increase of D_s with the increasing surface wetness in the monolayer region.

Interactions among the adsorbed molecules are not considered here, although they are existent. The inclusion of the interaction energy would slightly change the shape of the curve predicted by the modified Higashi model, but not the magnitude of D_s at $\theta = 1$[2,23,24].

Beyond-monolayer water coverage

Up to now we have neglected the flying time in considering the overall rate of diffusion. Flying time can be neglected only in the submonolayer region. In this region, the activated molecules

move freely and their speed is in the same order of a gas molecule. However, this is not true when the surface is more congested, or say, $\theta > 1$.

When all the surface sites are covered by one or more water molecules, the activated stearic acid molecule, during its flight; will encounter more collisions with water molecules and a considerable amount of steric hindrance. The enhanced steric hindrance is due to the formation of multilayer adsorption of water. And the collisions are encountered mainly with the activated (not totally desorbed) water molecules. These two factors could greatly slow down the flying molecules. When the flying time is longer than the site-holding time, the flying becomes rate-controlling. To make discussions easier, let us define two diffusion coefficients D_H and D_F, the first accounts for the site-holding time, the other accounts for the flying time. Thus, the overall diffusion coefficient, D_s, is given by the following equation:

$$\frac{1}{D_s} = \frac{1}{D_H} + \frac{1}{D_F} \qquad (23)$$

D_H dominates the overall diffusion rate in the sub-monolayer region, wherein D_F is negligible. When θ is beyond a monolayer, D_F becomes important, and eventually dominates when θ is great enough.

During the flight of the stearic acid molecule between sites, it experiences a retarding force due to the factors mentioned above. The true nature of the retardation is not known, but we may treat it as similar to that which a particle would have experienced if it were penetrating through a viscous medium with viscosity η. It is this viscosity, η, that we define as the "effective viscosity" of

the surface layer of water molecules in which the stearic acid molecule flies. Now let us consider this idea in terms of the more familiar Brownian diffusion in a bulk liquid.

The retarding force, the force required to move a sphere through a viscous medium at unit velocity, is given by Stokes's law,

$$f = 6\pi\eta r \tag{24}$$

where r is the radius of the sphere and η viscosity. Combining Stokes's law with Einstein's relation between the diffusion coefficient and the retarding force,

$$D = \frac{RT}{N \cdot f} \tag{25}$$

where R is molar gas constant, N Avogadro's number, T absolute temperature, the relation between diffusion coefficient and viscosity is obtained,

$$D = \frac{RT}{6\pi r N \eta} \tag{26}$$

Or we may write, for the motion in the surface layer with "effective viscosity" η_{eff}

$$D_F = \frac{RT}{6\pi r N \cdot \eta_{eff}} \tag{27}$$

In the experimental results of D_s vs. θ, D_s goes to a maximum at $\theta = 1$ and starts decaying. At this point, $1/D_F$ is no longer negligible as compared to $1/D_H$. When $\theta > 1$, $1/D_F$ becomes greater than $1/D_H$ and dominates the process. Meanwhile, it is reasonable to assume D_H to be a constant when $\theta > 1$, based on the fact that heat of adsorption

of water is rather constant in this region[21]. That is to say, the surface sites with one layer of water covered, are quite homogeneous energetically. For the purpose of interpreting the experimental results in the beyond-monolayer region where θ is not close to 1, this assumption does not have to be valid, since $1/D_H$ is negligible compared to $1/D_F$. Therefore, in the beyond-monolayer region,

$$\frac{1}{D_s} = \frac{1}{D_{H,\theta=1}} + \frac{6\pi r N \eta_{eff}}{RT} \tag{28}$$

As a crude approximation, we assume $D_{H,\theta=1} = D_{s,\theta=1}$, in order to obtain the dependence of η_{eff} on θ. Figure (16) is the plot of $\log_{10} \eta_{eff}$ against θ based on the experimental data of D_s as a function of θ and equation (28). Surprisingly enough, a straight line is obtained, which suggests:

$$\eta_{eff} \propto e^{k\theta} \tag{29}$$

where k can be calculated from the slope of the straight line in Figure (16).

This relation has a tempting formal similarity to the approximate theory of viscosity of liquids developed by Eyring and co-workers[25], which states

$$\eta \propto e^{\Delta G/RT} \tag{30}$$

where ΔG is molar "free energy of activation" required for a molecule to escape from its "cage" into an adjoining "hole". In our case, ΔG is somehow related to the energy required to overcome the steric hindrance and perhaps the attraction exerted by the water molecules.

If, this energy is proportional to the surface coverage of water, an exponential relation between η_{eff} and surface coverage should be expected.

It is also interesting to notice the analogy between equation (29) and the relation which accounts for the attenuation by scattering of a molecular beam:

$$I = I_o e^{-\sigma n \ell} \tag{31}$$

where σ is cross section, n the number density of scattering centers, ℓ the path length, I_o the initial flux and I the residual flux after scattering losses. In our context θ would be almost directly comparable with n.

Whatever the real mechanism, the "effective viscosity" of the surface water, η_{eff}, is the overall outcome of the retarding forces. It has been considered here only at a highly empirical level. Nevertheless, if it obeys equation (29), the experimental results shown in Figure (12) can be satisfactorily explained.

B. Stearic acid diffusion on KRS-5 at various surface wetnesses

KRS-5 is an amorphous mixture of thallium bromide and thallium iodide. The nature and the structure of its surface are not known, but it is presumed to have rather low heats of adsorption for polar molecules. Consequently, "site-bonding" would not be expected to have an important role in diffusion.

The relative rate of diffusion of stearic acid on the surface of KRS-5 at 40°C was measured as a function of the amount of adsorbed water. The results are shown in Table II and plotted in Figure (17). The exact values of surface diffusion coefficients were not calculated

since the boundary concentration, C_o, was not known. Monolayer coverage of water was estimated to be about 0.06 in absorbance at 3400 cm^{-1}. This estimation was based on the adsorption of water at a relative pressure of about 1/3 at 40°C, after the IRE was cleaned in the same way as it was done in the diffusion experiments.

TABLE II

Relative values of D_s for the system stearic acid - KRS-5 at various surface wetnesses at 40°C.

Absorbance at 3400 cm^{-1}	θ	slope of the plot of total material diffused vs. $\sqrt{t}$ i.e., $2C_o\sqrt{D_s/\pi}$, $\frac{abs}{\sqrt{sec}}$	relative values of D_s, in arbitrary units
0.032	0.53	3.145×10^{-5}	5.04
0.0815	1.35	3.145×10^{-5}	5.04
0.231	3.85	1.4×10^{-5}	1
0.64	10.66	1.54×10^{-5}	1.18

Some qualitative conclusions can be drawn from Figure (17) as follows. In the sub-monolayer region, D_s is roughly independent of the surface coverage of water. This implies that $\Delta E_1 = \Delta E_2$ in equation (11), and that the surface is energetically homogeneous. The condition that $\Delta E_1 = \Delta E_2$ also implies that the activation energies are the same for diffusion from a bare site and for diffusion from a water-covered site.

In the beyond-monolayer egion, D_s decreased five-fold when adsorbed water was increased about three-fold. Again, this can be interpreted as the outcome of the increase of flying time in

accordance with the ideas we invoked for the case of alumina. It is not intended here to analyze the dependence of the retardation on the surface coverage of water to the extent we did with alumina. However, it is expected that a similar relationship as on the alumina surface would be obeyed.

In passing, it should be mentioned that there is no way of predicting, from this study, the diffusion coefficient in a monolayer of stearic acid spread on the surface of water. This is due to the fact that, in our study, the diffusion takes place within the force field of the solid surface, while in the other case, it is more likely that a surface flow mechanism dominates the process. However, it is interesting to note that the reported value for this process is about of 10^{-6} cm^2/sec[26], of the same order as our experimental results for diffusion on a "wet" surface.

C. Discussion of some related work

(1) On the reduction of tungsten trioxide accelerated by platinum and water.

In the studies of the reduction of tungsten trioxide by hydrogen, carried out with mixtures of platinum black powder and tungsten trioxide; Benson, Kohn and Boudart reached the following conclusion[27]:

> "The reduction of WO_3 by H_2 to a blue form proceeds readily above 400°C. If the WO_3 powder is mixed with platinum black, reduction will start below 100°C. But if this mixture is made to adsorb water, reduction takes place rapidly at room temperature. The catalysis by platinum is apparently due to the dissociation of molecular hydrogen on the metal, followed by diffusion of adsorbed hydrogen atoms across the metal-oxide interface. The acceleration by water is ascribed to a marked increase in the rate of diffusion of the reducing species."

The amount of water adsorbed on the samples was not accurately measured, but it was approximated to be in the range of a monolayer[27]. Although the mechanism of the speeding up of the surface diffusion may be different in their case; for example, by exchange migration of a proton between adjacent water molecules, the effect of water is drastic. If the effect of the adsorbed water on the rate of diffusion of the "active" hydrogen is of the same character as in the system stearic acid - α alumina, that is, diffusion rate reaches a maximum at monolayer coverage of water, then their conclusion would be in strong agreement with the results of these studies. Indeed, water is powerful and mysterious!

(2). On surface diffusion of stearic acid on mica by counting the ^{14}C labelled acid.

Rideal and his co-worker measured the surface diffusion rate of stearic acid on mica (a silica-alumina), using a Blodgett film as the source. The measured diffusion coefficients are of one order of magnitude lower than the data obtained for the same system by Beischer[29].

Neither had reported the amount of water adsorbed on the mica surface. It is therefore suggested, based on the results of these studies, that the amounts of adsorbed water were different in the above two cases. Moreover, the great slope of the plot of $\log_{10} D_s$ vs. 1/T; hence an activation energy as high as 42 kcal/mole, may be due partially to the variation of the amount of adsorbed water caused by the varied temperatures.

4. Activation energy for surface diffusion

In order to obtain the activation energy for surface diffusion,

the surface coverage of water must be fixed, and the temperature varied. In this connection, D_s of stearic acid on (0001) surface of α alumina was measured at 27.6°C and 47°C, all at $\theta \cong 0.104$. Another value of D_s at 40°C may be extracted from Figure (12). These values of D_s are shown in Table III.

TABLE III

Values of D_s for stearic acid - (0001) α Al_2O_3 at various temperatures

temperature, °C	Absorbance at 3400 cm^{-1}	θ	D_s $cm^2/sec.$
27.6	0.103	1.128	2.86×10^{-6}
40	0.104	1.139	2×10^{-5}*
47	0.1042	1.141	4.08×10^{-5}

*value extracted from Figure (12) by interpolation

According to the Arrhenius equation,

$$D_s = D_o \cdot e^{-\Delta E/RT} \qquad (31)$$

values of $\log_{10} D_s$ were plotted against reciprocals of the absolute temperature (Figure 18). The activation energy of surface diffusion was calculated to be ca. 26 kcal/mole.

It should be noticed that the activation energy calculated here is at a surface coverage of water of a little more than a monolayer. It is, therefore, interpreted as the activation energy required for diffusion of stearic acid on <u>one layer</u> of adsorbed water molecules

on the solid surface.

For the diffusion on bare sites, the activation energy is expected to be higher than the figure given above. It is of interest to notice the rather high activation energy of 42 kcal/mole for diffusion of stearic acid on mica surface[28]. Although the amount of water adsorbed on the surface was not reported in that paper, it is specualted that the surface was "drier" than a monolayer.

CHAPTER V

SUMMARY AND CONCLUSIONS

In contrast to the indirect method of measuring surface diffusion coefficient by using porous materials, a direct method has been developed. In this method, internal reflection spectroscopy was applied coupled with the approximate solutions to the diffusion equation with pertinent boundary conditions.

An extension of Higashi's model of surface diffusion was made by allowing for the possibility of a finite sticking time on an occupied site, i.e., "second layer" adsorption. Compared to Higashi's model this model gives a better fit to various experimental data, and it does not blow up at monolayer coverage.

The effect of one species on the rate of surface diffusion of another species has been studied. In particular, a model system, stearic acid on (0001) surface of α alumina with absorbed water, has been ivestigated. The rate of surface diffusion was measured as a function of surface coverage of adsorbed water, θ. The diffusion coefficient is small at $\theta = 0.4$, increased by over two orders of magnitude as θ approaches one and decreased rapidly as θ is increased beyond one. The modified Higashi model and surface heterogeneity account for the increase in the sub-monolayer region, while a viscous mechanism was attributed for the decrease in the beyond-monolayer region.

When surface diffusion of the intermediates on the surfaces of the catalysts is the overall rate-controlling step, the vapor pressure

of water in the reactor should be adjusted, such that the amount of adsorbed water corresponds to the maximum rate of surface diffusion of the intermediates. The overall reaction is therefore "catalyzed" by water.

Appendix 1

Solution for diffusion equation

The governing equation

$$\frac{\partial C}{\partial t} = D\frac{\partial^2 C}{\partial x^2} \tag{1}$$

The boundary conditions for constant source diffusion

$$x=0, \quad C=C_0 \tag{2}$$

$$x=b, \quad \frac{\partial C}{\partial x}=0 \tag{3}$$

$$t=0, \quad C=0 \tag{4}$$

Taking Laplace transform of eq. (1)

$$s\cdot F(x,s) - C(x,0) = D\frac{\partial^2 F}{\partial x^2} \tag{5}$$

here $F(x,s)=\mathcal{L}\{C(x,t)\}$ and $C(x,0)=0$ from eq. (4).

General solution for eq. (5)

$$F(s,x) = A(s)\cdot e^{\sqrt{s/D}\cdot x} + B(s)\cdot e^{-\sqrt{s/D}\cdot x} \tag{6}$$

$$\frac{\partial F}{\partial x} = A(s)\cdot e^{\sqrt{s/D}\cdot x}\sqrt{\frac{s}{D}} - B(s)\cdot e^{-\sqrt{s/D}\cdot x}\sqrt{\frac{s}{D}}$$

From equation (3)

$$0 = e^{\sqrt{s/D}\cdot b}\left(\sqrt{\frac{s}{D}}\cdot A(s)\right) - e^{-\sqrt{s/D}\cdot b}\left(B(s)\cdot\sqrt{\frac{s}{D}}\right)$$

$$\therefore B(s) = A(s)\cdot e^{2\sqrt{s/D}\cdot b} \qquad (7)$$

From equation (2)

$$x=0, \quad F = C_0/s$$

$$\therefore F(o,s) = C_0/s = A(s) + B(s) \qquad (8)$$

Solving equations (7) and (8)

$$A(s) = \frac{C_0/s}{1+e^{2\sqrt{s/D}\cdot b}}$$

$$B(s) = \frac{C_0/s\cdot e^{2\sqrt{s/D}\cdot b}}{1+e^{2\sqrt{s/D}\cdot b}}$$

Substitute $A(s)$ and $B(s)$ into eq. (6)

$$F(s,x) = \frac{C_0}{s}\cdot\frac{e^{\sqrt{s/D}\cdot x} + e^{-\sqrt{s/D}\cdot(x-2b)}}{1+e^{2\sqrt{s/D}\cdot b}}$$

$$= \frac{C_0}{s}\cdot\frac{e^{\sqrt{s/D}(x-2b)} + e^{-\sqrt{s/D}\cdot x} - e^{\sqrt{s/D}(x-4b)} - e^{-\sqrt{s/D}(x+2b)}}{1-e^{-4\sqrt{s/D}\cdot b}}$$

and since

$$\frac{1}{1-e^{-4\sqrt{s/D}\cdot b}} = 1+e^{-4b\sqrt{s/D}}+e^{-8b\sqrt{s/D}}+e^{-12b\sqrt{s/D}}+\cdots\cdots$$

$$\therefore F(s,x)=\frac{C_o}{s}\Big[e^{\sqrt{s/D}\,(x-2b)}+e^{\sqrt{s/D}\,(x-6b)}+e^{\sqrt{s/D}\,(x-10b)}+\cdots\cdots$$
$$-e^{\sqrt{s/D}\,(x-4b)}-e^{\sqrt{s/D}\,(x-8b)}-e^{\sqrt{s/D}\,(x-12b)}-\cdots\cdots$$
$$+e^{-\sqrt{s/D}\cdot x}+e^{-\sqrt{s/D}\,(x+4b)}+e^{-\sqrt{s/D}\,(x+8b)}+\cdots\cdots$$
$$-e^{-\sqrt{s/D}\,(x+2b)}-e^{-\sqrt{s/D}\,(x+6b)}-e^{-\sqrt{s/D}\,(x+10b)}+\cdots\cdots\Big]$$

Upon taking the inverse Laplace transfrom and note that

$$\mathcal{L}^{-1}\left\{\frac{e^{\sqrt{s}\cdot a}}{s}\right\} = 1-\operatorname{erf}\sqrt{\frac{a^2}{4t}} = \operatorname{erfc}\sqrt{\frac{a^2}{4t}}$$

The solution is obtained

$$C(x,t)=C_o\Big[\operatorname{erfc}\frac{x-2b}{\sqrt{4Dt}}+\operatorname{erfc}\frac{x-6b}{\sqrt{4Dt}}+\operatorname{erfc}\frac{x-10b}{\sqrt{4Dt}}+\cdots\cdots$$
$$-\operatorname{erfc}\frac{x-4b}{\sqrt{4Dt}}-\operatorname{erfc}\frac{x-8b}{\sqrt{4Dt}}-\operatorname{erfc}\frac{x-12b}{\sqrt{4Dt}}-\cdots\cdots$$
$$+\operatorname{erfc}\frac{-x}{\sqrt{4Dt}}+\operatorname{erfc}\frac{-(x+4b)}{\sqrt{4Dt}}+\operatorname{erfc}\frac{-(x+8b)}{\sqrt{4Dt}}+\cdots\cdots$$
$$-\operatorname{erfc}\frac{-(x+2b)}{\sqrt{4Dt}}-\operatorname{erfc}\frac{-(x+6b)}{\sqrt{4Dt}}-\operatorname{erfc}\frac{-(x+10b)}{\sqrt{4Dt}}-\cdots\cdots\Big]$$

APPENDIX 2

REVIEW OF THE STRUCTURING EFFECT OF SURFACE ON WATER

The effect of interface on the structure of a liquid and its effective range has been a puzzle to scientists. Owing to experimental difficulties, the evidences of long range surface forces and deep surface orientation effect are still skeptical.

Among the interfacial liquids, water has been observed the most. We are interested in trying to "see" whether there is any structural ordering of water at or near solid interfaces. The evidences and hypotheses for such structuring have been recently discussed in some detail by Drost-Hansen[39]. In particular, we have been curious about the interface with the polar groups of the compressed monomolecular films of substance like stearic acid and cetyl alcohol.

We have been able to obtain the x-ray pattern of a 20 microns thick water film with stearic acid or oleic acid compressed monolayer on its surface. The patterns showed no difference from those of bulk water at the same temperatures.

To reduce the range of observation, we adopted the technique of internal reflection infrared spectroscopy which under our conditions gives a penetration depth of the order of fractions of a micron. The prism used in this technique is called an "internal reflection element" or IRE.

Two layers of calcium stearate were deposited on a germanium IRE by the method of Langmuir and Blodgett, the polar groups of the first layer being inward and attached to the solid surface and those of the second layer being outward and immersed in water. The IR

spectra were taken and showed two layers of stearates and a water band which is identical with normal bulk water. This result draws the conclusion that if the compressed and oriented polar groups of stearate monolayer have any structural ordering effect on neighboring water at all, the range is negligibly smaller than a micron.

Some attempts have been made for the vicinal water structure on germanium surface, fused quartz surface, AgCl surface, with IRE made of these materials. The spectrum of a water film of about 3 microns thick sandwiched between a germanium IRE and a freshly splitted mica film was also taken.

None of them showed any difference from the normal bulk water. Therefore in any attempt to further study the surface effect on water by spectroscopy, it is recommended to concentrate on the few molecular layers of adsorbed water on solid surfaces.

APPENDIX 3

ADSORPTION FROM SOLUTION

One of the standard methods of measuring surface area of a fine powder is based upon the adsorption of a suitable acid from solution. This method is the direct outcome of an assumption made by Harkins and Gans[33]. In the adsorption of acids from their solutions on to a solid surface, they assumed that: (a) at maximum adsorption the surface is covered by a close-packed oriented monolayer, and (b) the area occupied by each molecule is the same as on an aqueous surface - that is, approximately 20 $\mathring{A}^2$. Experimental supports of this assumption on various adsorption systems have been given in the past four decades since Harkins's assumption was made.

Harkins et al. studied the adsorption of oleic acid from its benzene solution on to TiO_2 surface[33]. At concentrations above 0.01 to 0.02 mole per kilogram of benzene, the adsorption of oleic acid became practically constant. This maximum adsorption was found to be equivalent to the amount of a condensed monolayer on the surface of the grains of powder. They further proved the above conclusion in their studies of the flocculation of the titanium oxide powder in the benzene solution of oleic acid[34]. They also postulated that the monolayer was orientated with the polar end of the molecule next to the solid surface. Ewing[35] chose zinc oxide to be the adsorbent powder and some aliphatic chain esters to be the adsorbate. the solvent for the esters was benzene. The specific surface area of the zinc oxide powder calculated based on the Harkins assumption from the adsorption measurements agreed closely with the surface area

calculated by the photomicrographic method. Furthermore, he found that the glycol dipalmitate molecule covered twice as large an area as the methyl stearate molecule did. Adsorption of stearic acid on metal surfaces was determined by Greenhill[36]. Harkins's assumption was supported by the agreement between the surface areas calculated based upon this assumption and from the mean diameter of the spherical particles for an iron powder. The powders of nickel, silver and copper were also studied, but no calculations were made owing to the very irregular nature of the particles. In his work on ionic crystals[37], Hutchingson used Harkins's assumption to measure the surface area of a sodium fluoride powder, based upon the maximum adsorption of stearic acid.

The orientation of the adsorbed stearic acid molecules (from its CCl_4 solution) on zinc oxide surface was studied by Hasegawa and Low[38]. It appeared that the monolayer film was orientated in such a way that the hydrocarbon chains were in a coplanar, trans zigzag mode, and prbably tilted about 60^{o}.

The most accepted belief at the present time is that for highly polar surfaces, such as those of metal oxides, the maximum adsorption of n-fatty acids from their solutions in nonpolar solvents corresponds to a compressed monolayer in quantity. For weakly polar surfaces, such as those of ionic crystals and semi-conductors, no work seems to have been done in regards to Harkins's assumption. Furthermore, the very limited knowledge about the orientation of the adsorbed molecules[38] demands more information in the literature.

We took advantage of the recently developed techniques of internal reflection spectroscopy (IRS) to study the adsorption of stearic acid from its solution in CCl_4 on to a semiconductor surface, i.e., germanium

surface. The observations were made in situ owing to the good index matching[12b] of this system. The maximum amounts of adsorption from two solutions were measured: 1.4×10^{-4} M stearic acid in CCl_4 (solution A) and 9.3×10^{-3} M stearic in CCl_4 (solution B). The adsorption was measured in terms of absorbance at the peak of the asymmetric stretching band (2928 cm^{-1}) of the methylene groups and the absorbance was then compared with the absorbance due to a Blodgett deposited monolayer. The germanium plate was cleaned with warm chromic acid and followed by HNO_3 and flushed with distilled water. The treatment with HNO_3 was to ensure the displacement of residual chromium ions. The absorption spectra of the adsorbed stearic acid were also recorded by using the polarized radiations. The possibility of measuring the orientation of the adsorbed molecules with the polarized spectra has been shown by Haller and Rice[13].

The absorbance of a calcium stearate compressed monolayer on a sapphire surface was measured as 0.4 (logarithm based on 10) at the peak of the C-H asymmetric stretching[13]. The number of reflections (at 45°) for the sapphire plate being used was 100. In our experiments, a germanium plate with 25 reflections (at 45°) was used. In order to obtain the monolayer absorbance from the available data, a conversion from the sapphire system to the germanium system had to be made. The conversion was done as follows.

$$\frac{A_{\text{sapphire-stearate-air}}}{A_{\text{germanium-stearate-}CCl_4}} \approx \frac{\frac{n_{st.}}{n_{sap}}\left[1-\left(\frac{n_{CCl_4}}{n_{Ge}}\right)^2\right]}{\frac{n_{st.}}{n_{Ge}}\left[1-\left(\frac{n_{air}}{n_{sap}}\right)^2\right]} = 3.043$$

Here A is absorbance and n the index of refraction. Thus, monolayer absorbance for our system was 0.0757 (log. based on e).

The maximum amount of adsorption from solution A was 0.0328 (after 16 hrs of adsorption), and was 0.0312 from solution B (after 80 hrs. of adsorption). This amount can be considered as the maximum amount of adsorption and there should not be any more adsorption at higher concentrations of the solution. Assuming that the absorbance due to methylene groups is the same for calcium stearate and stearic acid, the maximum adsorption on germanium surface corresponds to about 1/2 of a compressed monolayer.

The spectra at the maximum absorption were also recorded by using the perpendicular and parallel polarized lights. The perpendicular to parallel absorbance ratio, $A_{\perp}/A_{||}$, for the asymmetric methylene stretch is 0.526. This value is for the adsorption from solution B, polarized spectra were not recorded for the adsorption from solution A. The calculated ratio for the completely random orientation of the hydrocarbon chains is 0.529. For an ideally oriented monolayer, i.e., the C-H bonds in the methylene groups are parallel to the substrate surface, the ratio is 1.183. (The calculation of these ratios was illustrated by Haller et al.[13].) Therefore, the adsorbed stearic acid molecules on the germanium surface were randomly oriented.

Some experiments were also done on the alumina surface. Owing to the poor index matching[12b], the radiation was totally absorbed by the CCl_4 solution. Therefore, after the maximum adsorption was completed, (which took several hours) and upon removal from the solution, the alumina plate was immediately dipped in solvent for

several timesin order to remove the clinging excess solution. The plate was then drained and dried. The spectra of the adsorbed molecules were then recorded. It should be noted that the amount of adsorbed material survived the dipping did not necessarily correspond to the amount which was adsorbed. We were thus only interested in the orientation of the adsorbed molecules after the dipping.

The adsorption of stearic acid from its CCl_4 solution (10^{-2}M) on (0001) α Al_2O_3 was studied. After two hours of adsorption, the plate was removed from the solution and dipped in CCl_4. The amount of stearic acid remained on the surface depended upon the number of dips. After two dips the amount was equivalent to a compressed monolayer. The ratio of the perpendicular to parallel absorbance at 2920 cm^{-1} for the surviving stearic acid molecules was 1.622. The ratios for the two extreme orientations are: 1.28 for completely random and 2.13 for ideally-close packed. The measured value of 1.622 suggests that there is a certain degree of orientation for the dipping-survived molecules. Without the dipping and draining processes, the adsorbed molecules are expected to be more orientated.

From the results of the experiments mentioned above, it appears that Harkins's assumption does not apply to the kind of surfaces like germanium. Instead, the maximum amount of adsorption is less than a monolayer and the adsorbed molecules are randomly oriented. For the metal oxide surfaces, like alumina, the orientation of the adsorbed n-fatty acid molecules appears to exist.

REFERENCES

1. McIntosh, J.R., "Surface Diffusion in Microporous Media at High Surface Coverage", Ph.D. Thesis, University of Iowa (1966).

2. Higashi, K., Ito, H. and Oishi, J., J. Atomic Energy Soc. (Japan) 5, 846 (1963).

3. Carman, C.P., "Flow of Gases through Porous Media", Academic Press (1956).

4. Reed, E.M., "Surface Diffusion of Gas Mixtures in Porous Materials", Ph.D. Thesis, Yale University (1969).

5. Hill, T.L., J. Chem. Phy., 25, 730 (1956).

6. Carman, P.C. and F.A. Raal, Proc. Roy. Soc., A209, 38 (1951).

7. Gilliland, E.R., Baddour, R.F. and Russell, J.L., A. I. Ch. E. Journal, 4, 90 (1958).

8. Perkingson, G.P., "Flow of Adsorbed Gases through Microporous Media", Ph.D. Thesis, MIT (1965).

9. Hwang, S.T., "Surface Diffusion in Microporous Media", Ph.D. Thesis, University of Iowa (1965).

10. Reyes, R.R., "A Non-equilibrium Statistical Mechanical Model for Surface Diffusion", Ph.D. Thesis, University of Michigan (1966).

11. Ross, J.W. and R.J. Good, J. of Phy. Chem., 60, 1167 (1956).

12. (a) Lorrain, P. and D. Corson, "Electromagnetic Fields and Waves", W.H. Freeman and Company, San Francisco, California (1970).

    (b) Harrick, N.J., "Internal Reflection Spectroscopy", Interscience, New York, N.Y. (1967).

13. Haller, G.L. and R.W. Rice, J. of Phy. Chem., 74, 4386 (1970).

14. Blodgett, K.B., J. Am. Chem. Soc., 57, 1007 (1935).

15. Wexler, A.S., App. Spect. Review, 1(1), 29 (1967).

16. Bassett, G.A., Proceedings of the International Symposium on Condensation and Evaporation of Solids, E. Rutner, P. Goldfinger and J.P. Hirth, Eds. (Gordon and Breach, Science Publishers, Inc., New York, 1964) p. 599.

17. Reiss, H., J. App. Phy., 39, 5045 (1968).

18. Gregg, S.J. and K.S.W. Sing, "Adsorption, Surface Area and Porosity", Academic Press (1967), p. 49.

19. Brunaner, S., L.S. Deming, W.S. Deming and E. Teller, J. Am. Chem. Soc., 62, 1723 (1940).

20. Haller, G.L. and R.W. Rice, Private communication.

21. Yao, Y.-F.Y., J. Phys. Chem., 69, 3930 (1965).

22. Armistead, C.G., A.J. Tyler and J.A. Hockey, Trans. Faraday Soc., 67, 500 (1971).

23. Fowler, R.H. and E.A. Guggenheim, "Statistical Thermodynamics", Cambridge Univ. Press (1965), Chapter 10.

24. Hill, T.L., J. Chem. Phy., 14, 268 (1946).

25. Glasstone, S., K.J. Laidler and H. Eyring, Theory of Rate Processes, McGraw-Hill, New York (1941), Chapter 9.

26. Good, P.A. and R.S. Schechter, 69th A.I.Ch.E. National Meeting, Cicinnati, Ohio, May 1971, Paper number 31b.

27. Benson, J.E., H.W. Kohn and M. Boudart, J. Catalysis, 5, 307 (1966).

28. Sir Eric Rideal and J. Tadayon, Proc. Roy. Soc. (London), A225, 357 (1954).

29. Beischer, D.E., U.S. Naval School of Aviation Medicine Naval Air Station, Pensacola, Florida, Proj NM 001 059.16.07. (1951).

30. (a) Blodgett, K.B. and I. Langmuir, Physical Review, 51, 964 (1937).

(b) Langmuir, I. and V.J. Schaefer, J.A.C.S., 58, 284 (1936).

(c) Spink, J.A. and J.V. Sanders, Trans. Faraday Soc., 51, 1154 (1955).

31. (a) Frech, R.E., "Optical Constants of Crystals and Aqueous Solutions by A.T.R. Techniques", Ph.D. Thesis, University of Minnesota (1968).

(b) Thompson, W.K., Trans. Faraday Soc., 61.2, 2635 (1965).

(c) Corkill, Goodman, Ogden, and Tate, Proc. Roy. Soc., A273, 84 (1963).

32. Newnham, R.E. and Y.M. DeHann, Z. Kristallogr., 117, 235 (1962).

33. Harkins, W.D. and D.M. Gans, J.A.C.S., 53, 2804 (1931).

34. Harkins, W.D. and D.M. Gans, J. Phys. Chem., 36, 86 (1932).

35. Ewing, W.W., J.A.C.S., 61, 1317 (1939).

36. Greenhill, E.B., Trans. Farad. Soc., 45, 625 (1949).

37. Hutchingson, E., Trans. Farad. Soc., 63, 443 (1947).

38. Hasegawa, M. and M.J.D. Low, J. Colloid and Interface Sci., 29, 593 (1969).

39. Drost-Hansen, W., I&EC, 61, 10 (1969).

TABLE OF FIGURES

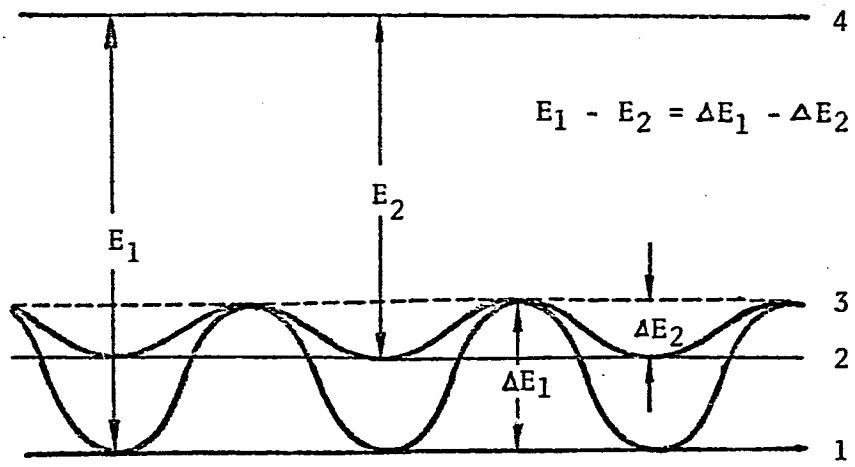

1. Energy of adsorbed molecules in the first layer.

2. Energy of adsorbed molecules in the second (and higher ordered) layers.

3. Energy level for diffusion.
   (also energy level of molecules in the second layer in Higashi's model)

4. Energy of gaseous molecules.

ENERGY DIAGRAM FOR A HOMOGENEOUS SURFACE

FIG. 1

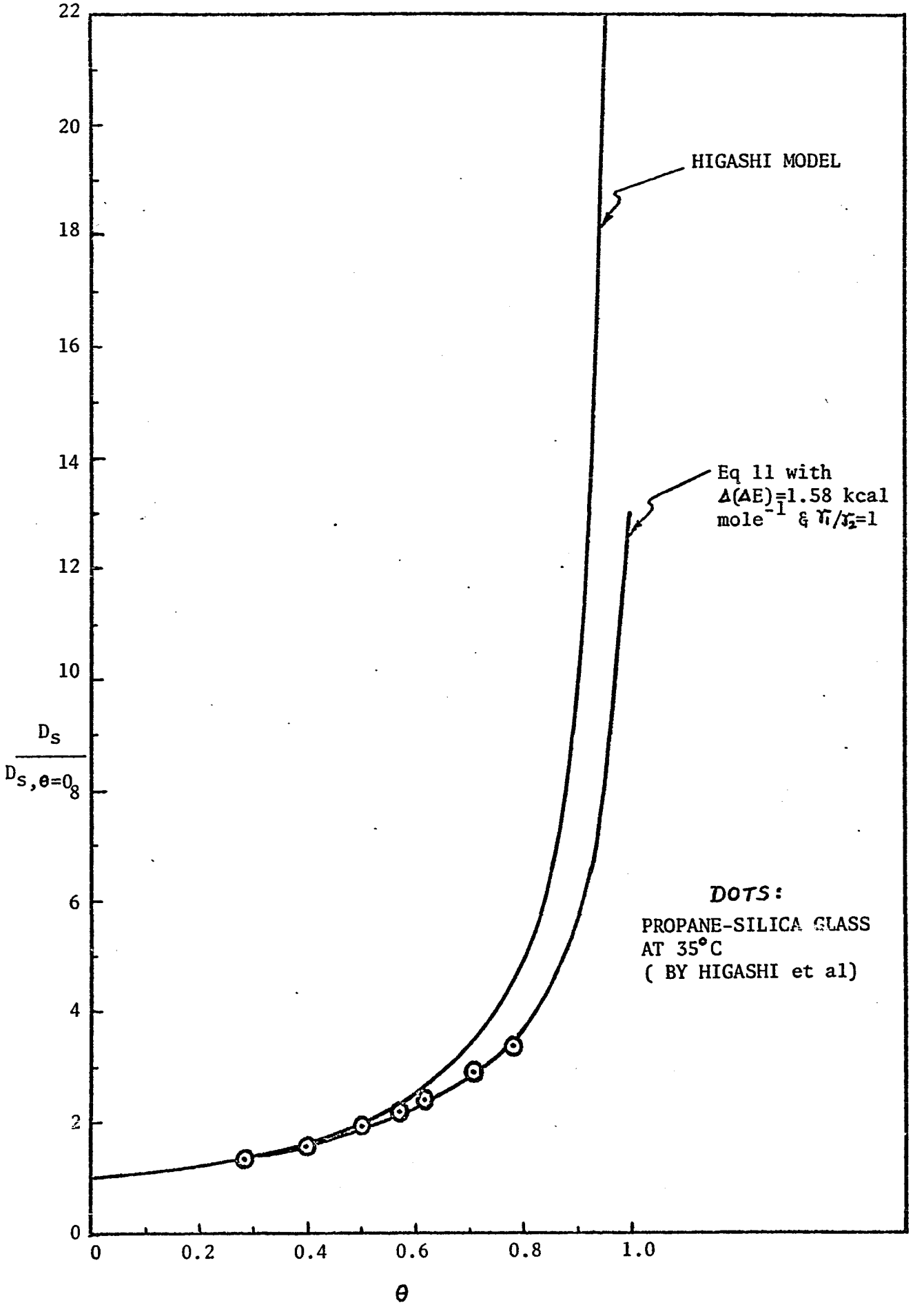

FIG 2

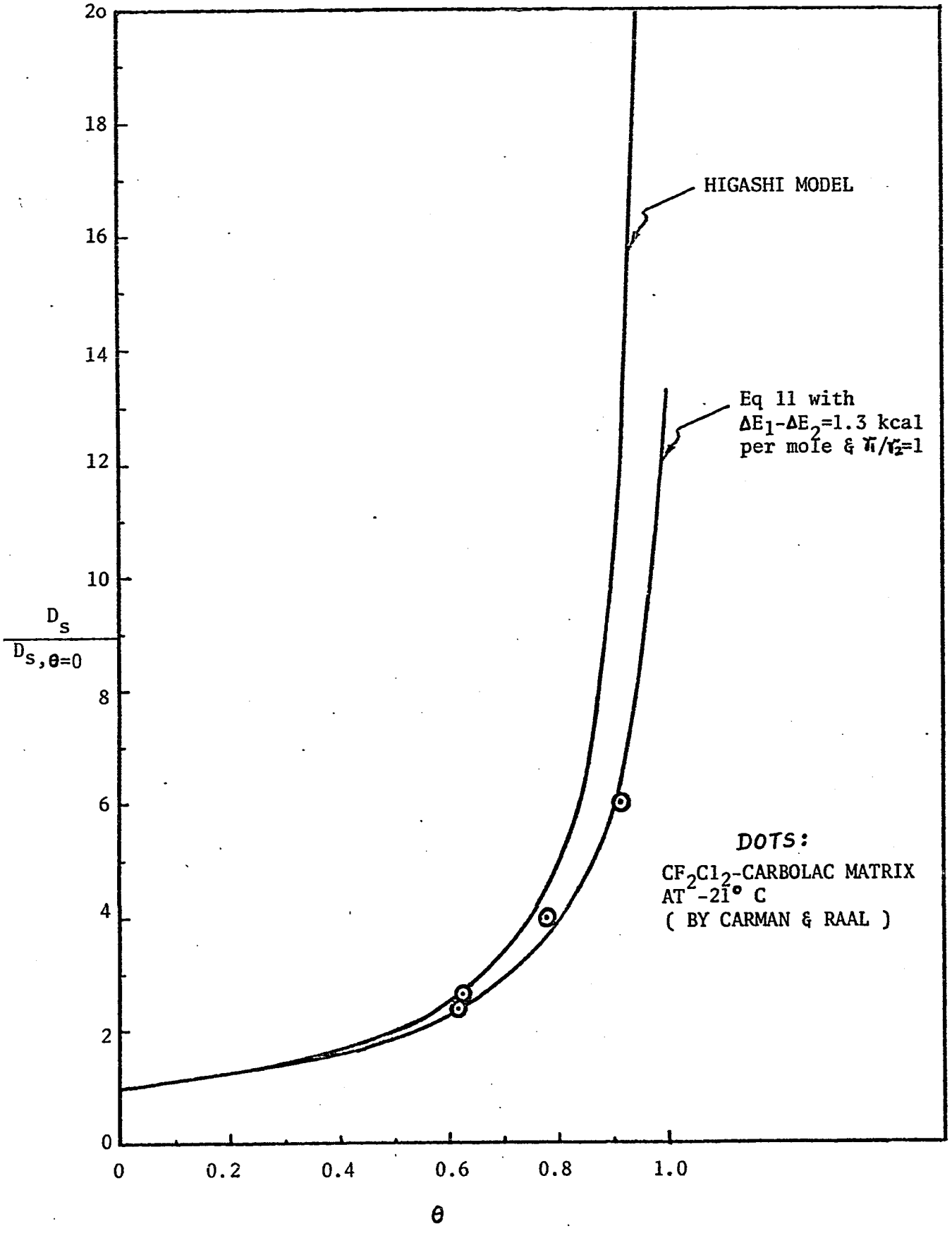

FIG 3

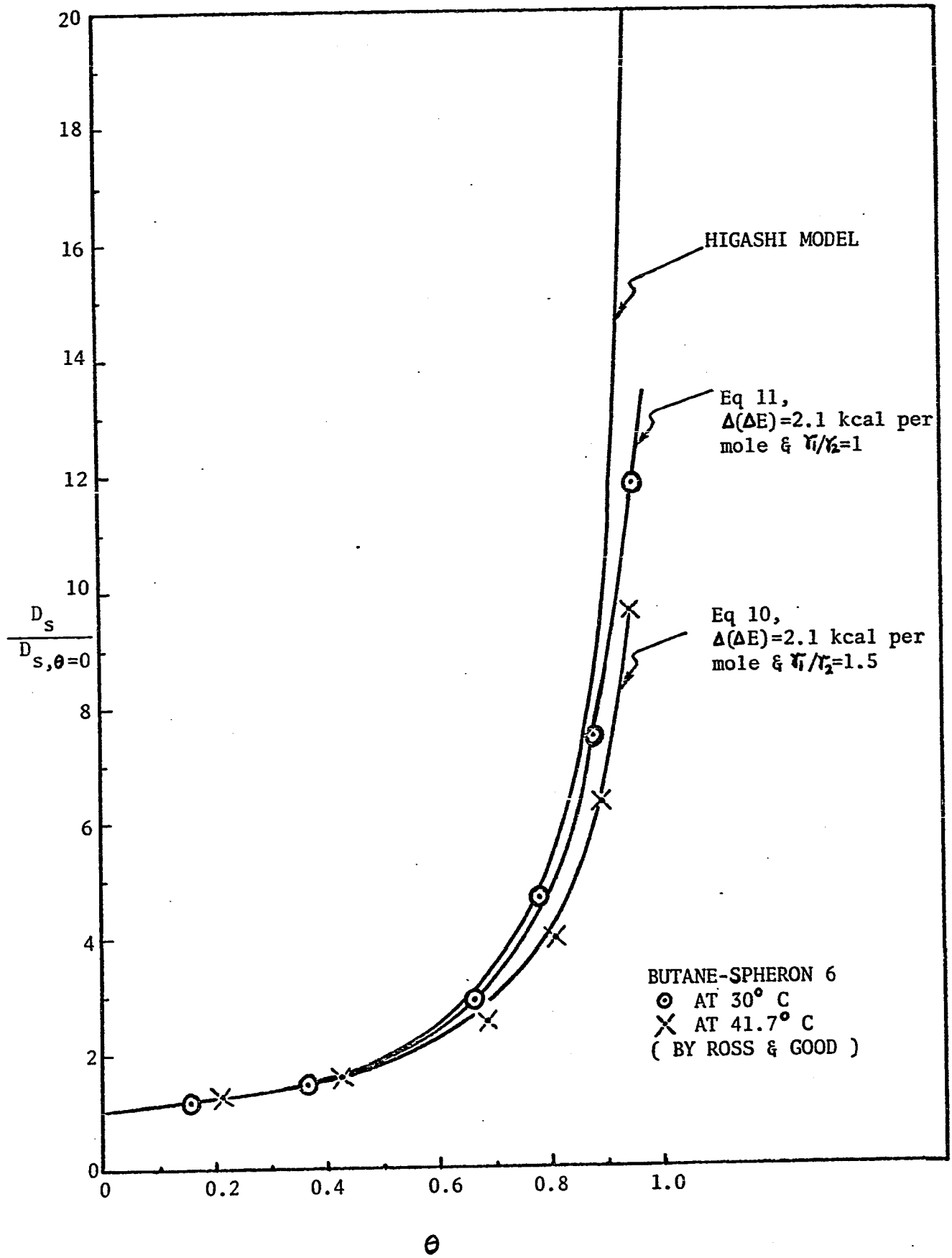

FIG 4

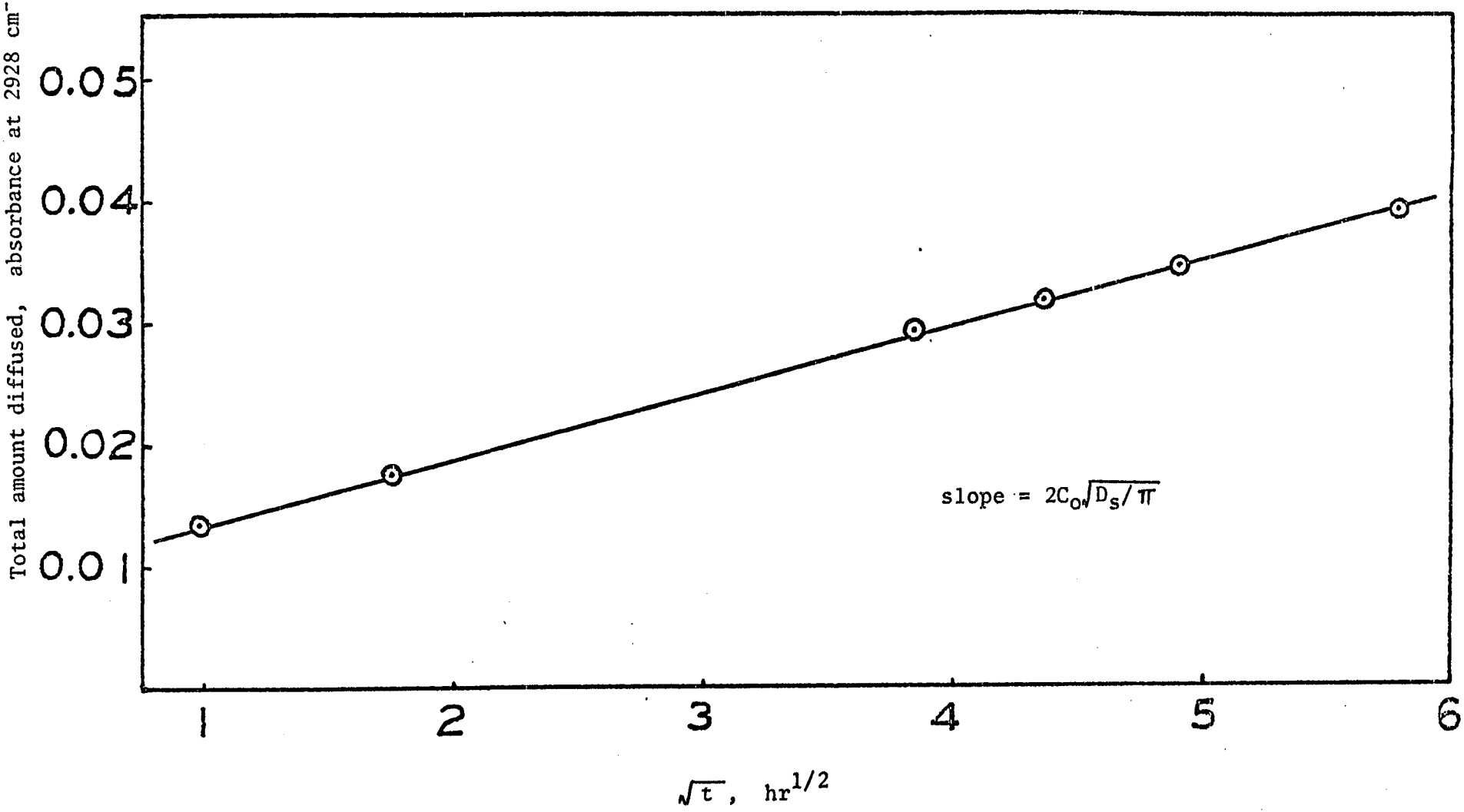

FIG 5

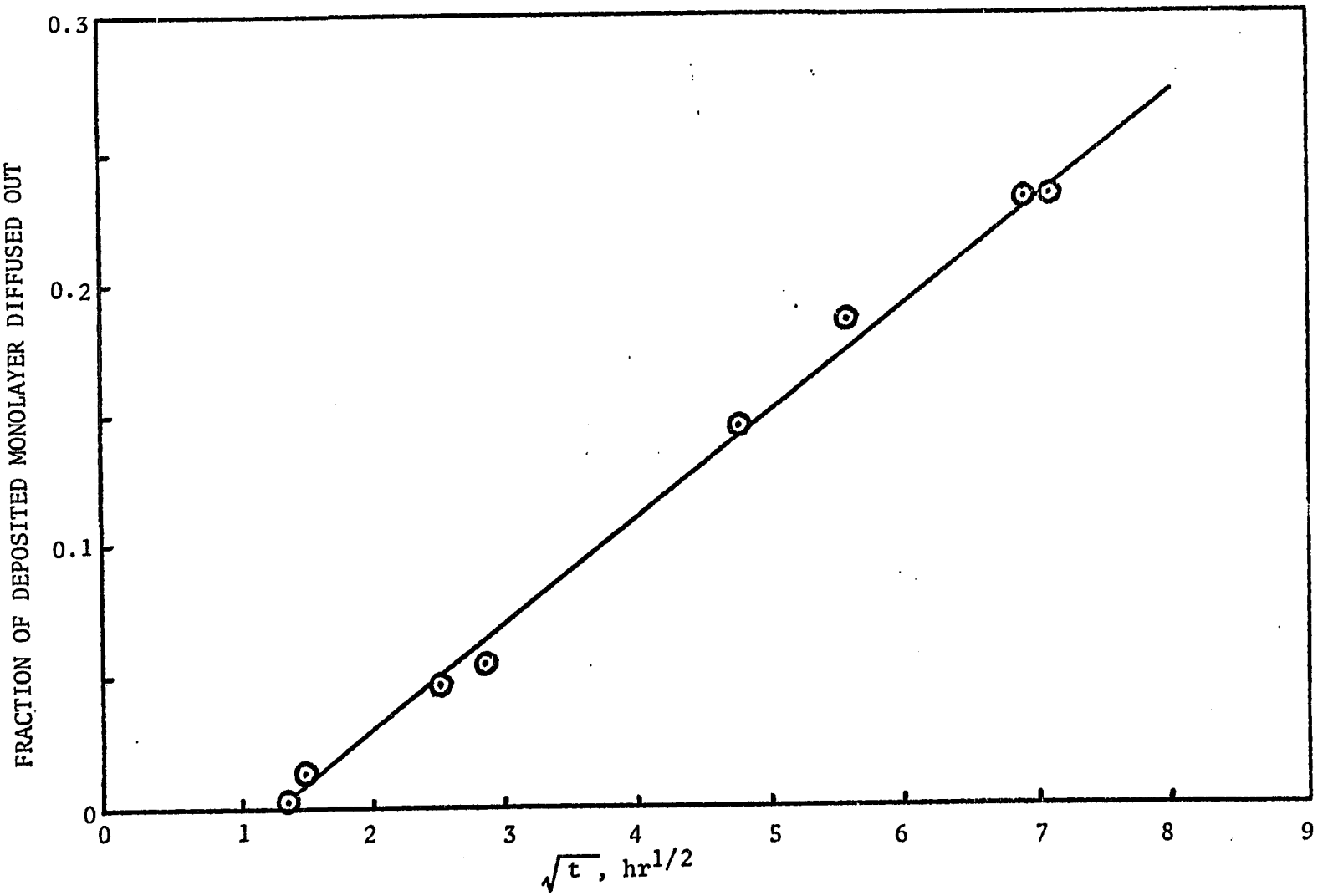

FIG 6

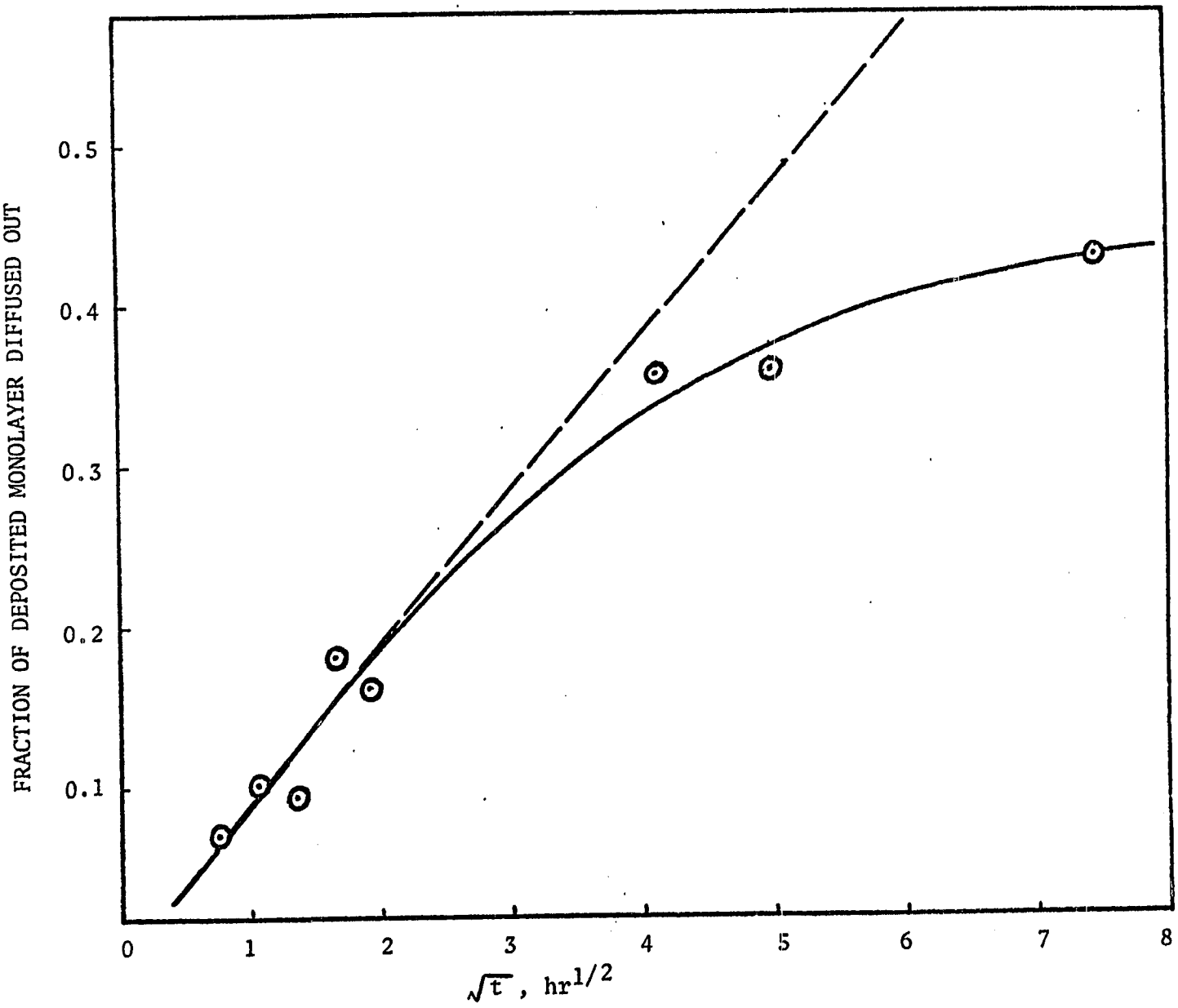

FIG 7

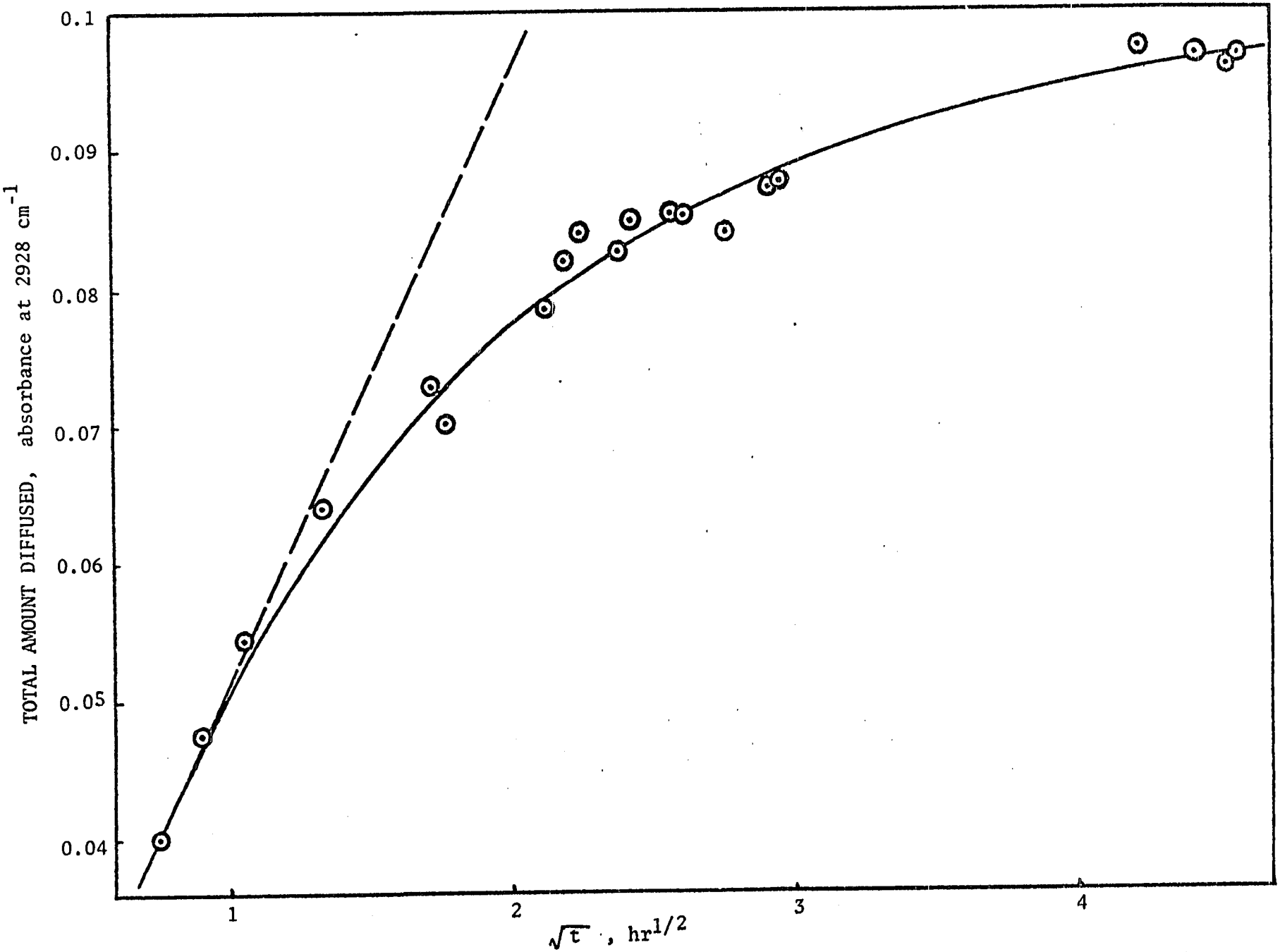

FIG 8

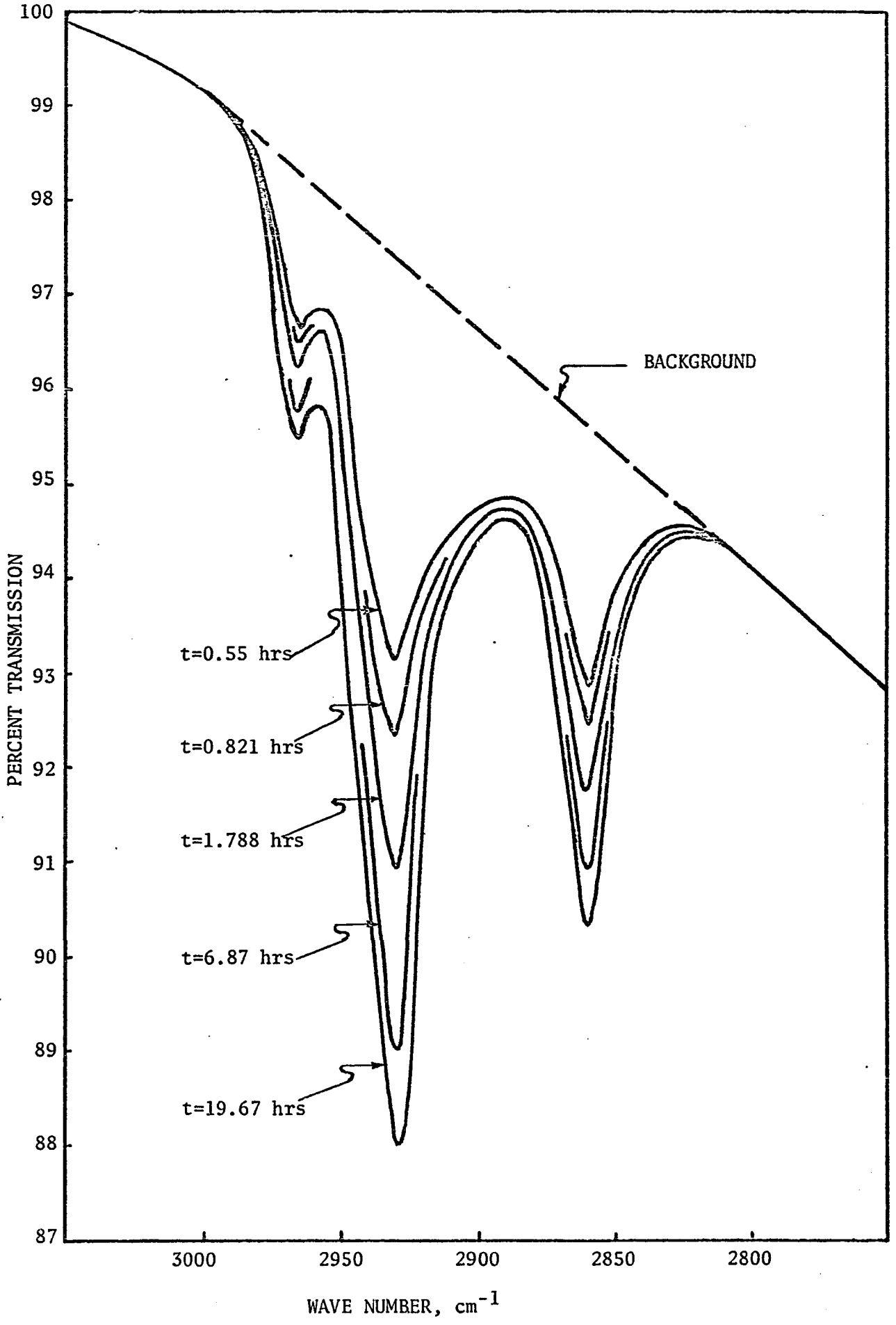

FIG 9

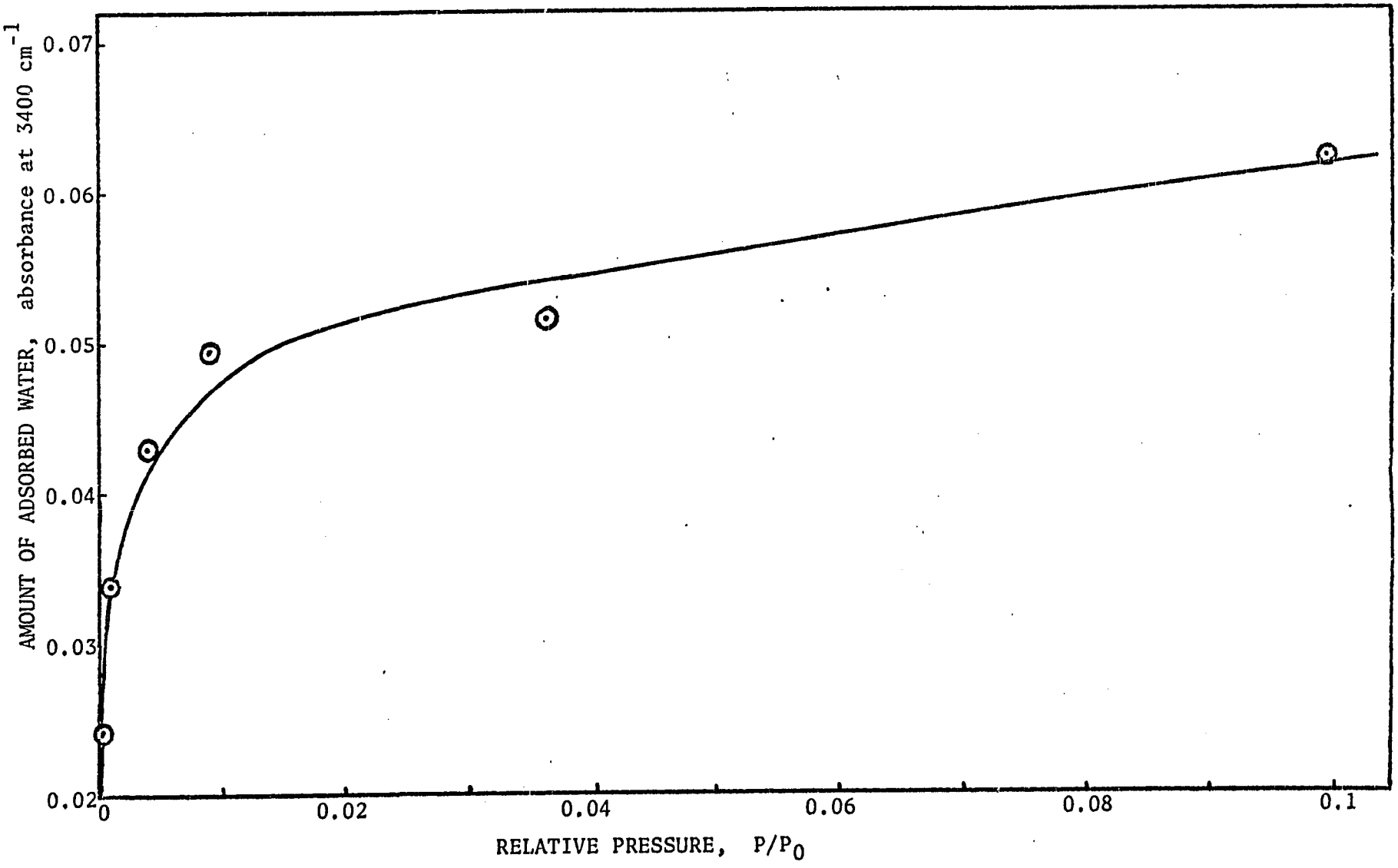

FIG 10

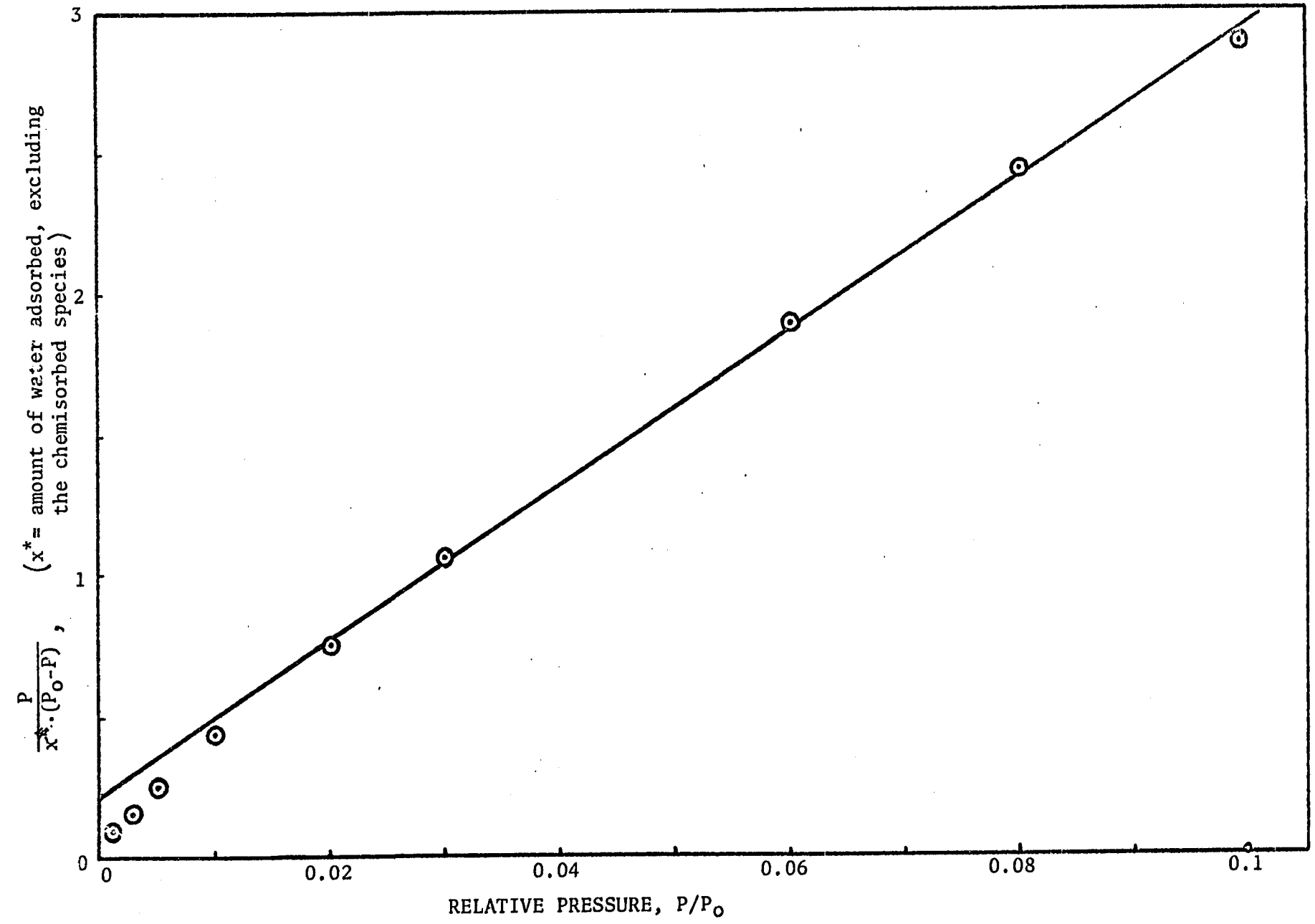

FIG 11

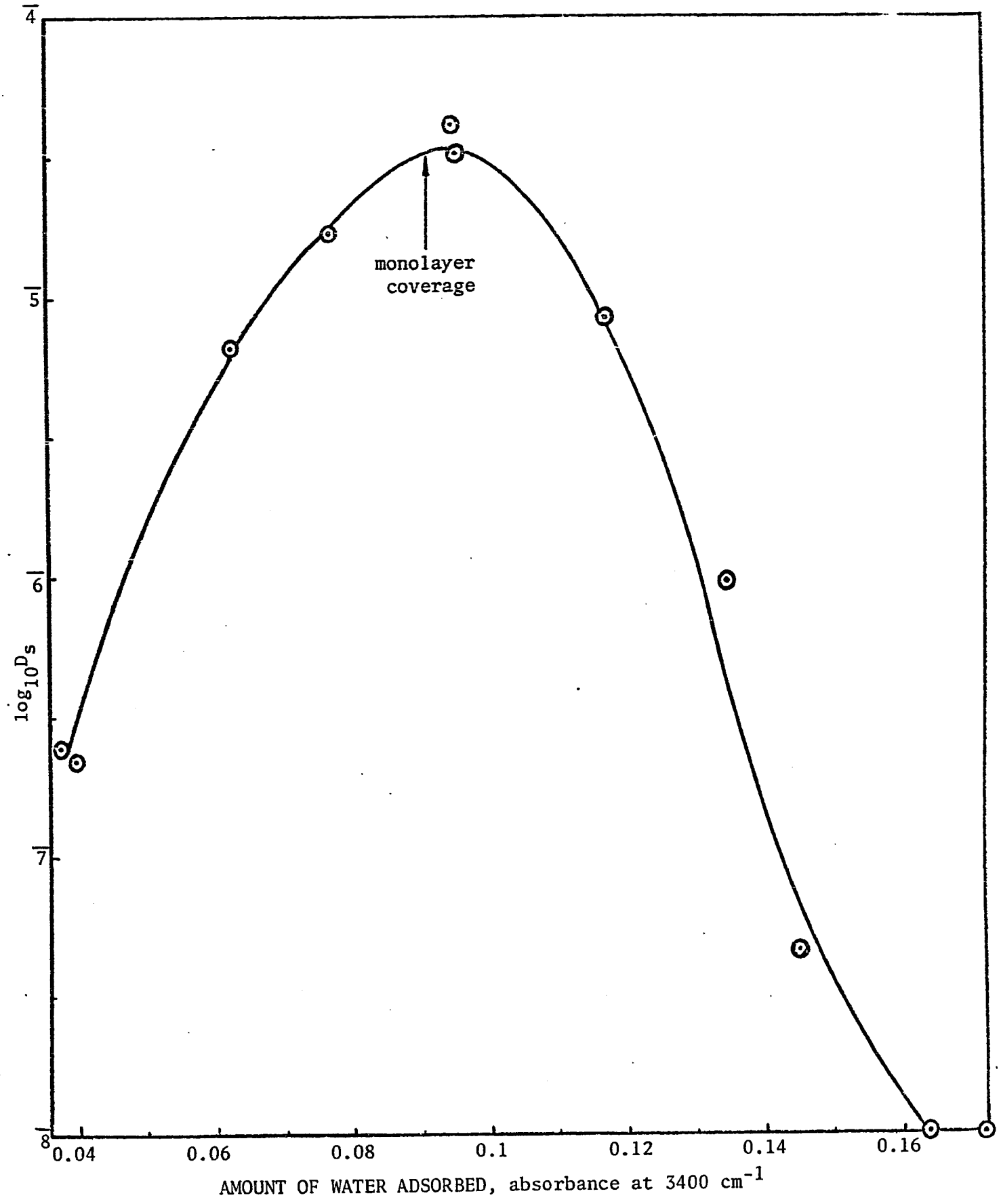

FIG 12

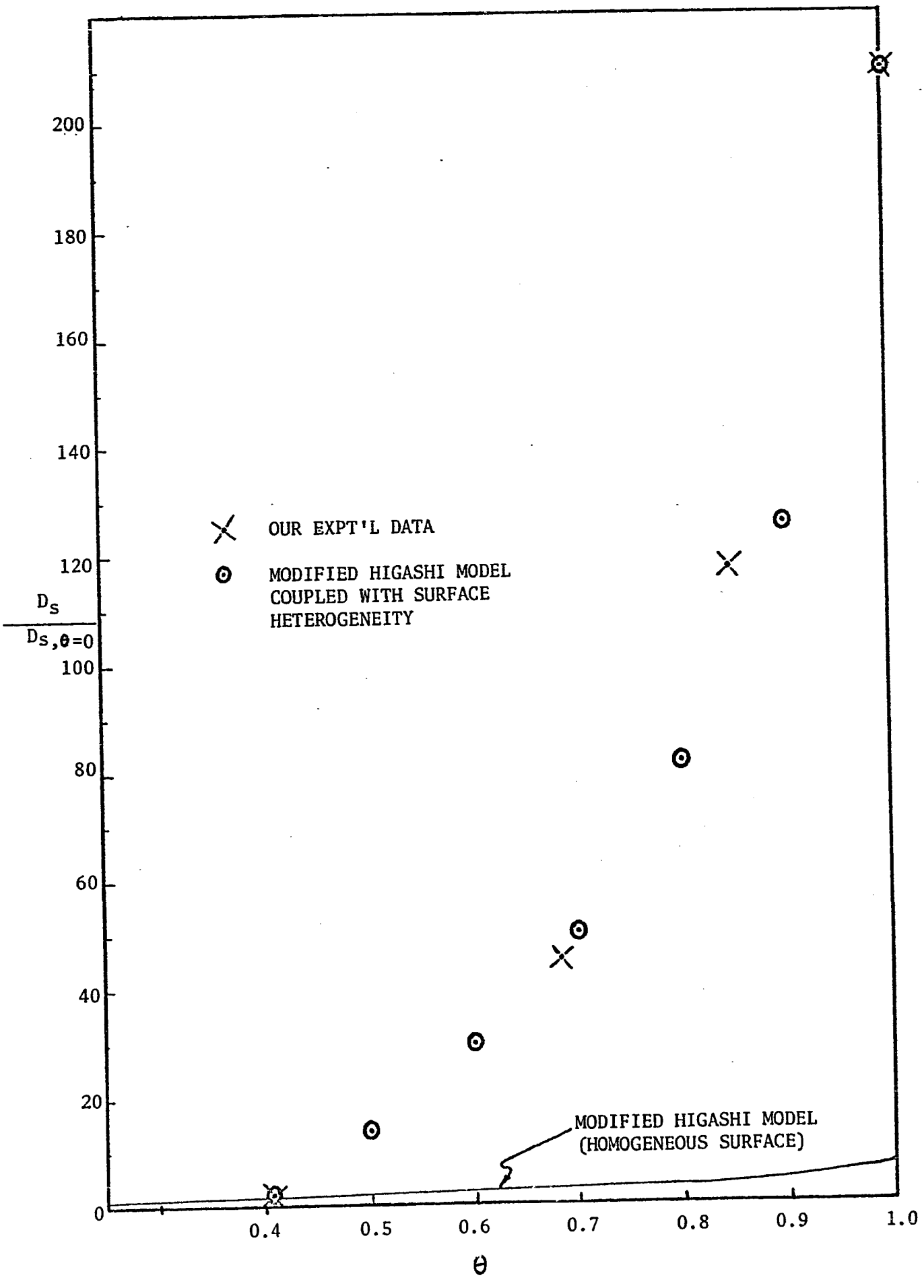

FIG 13

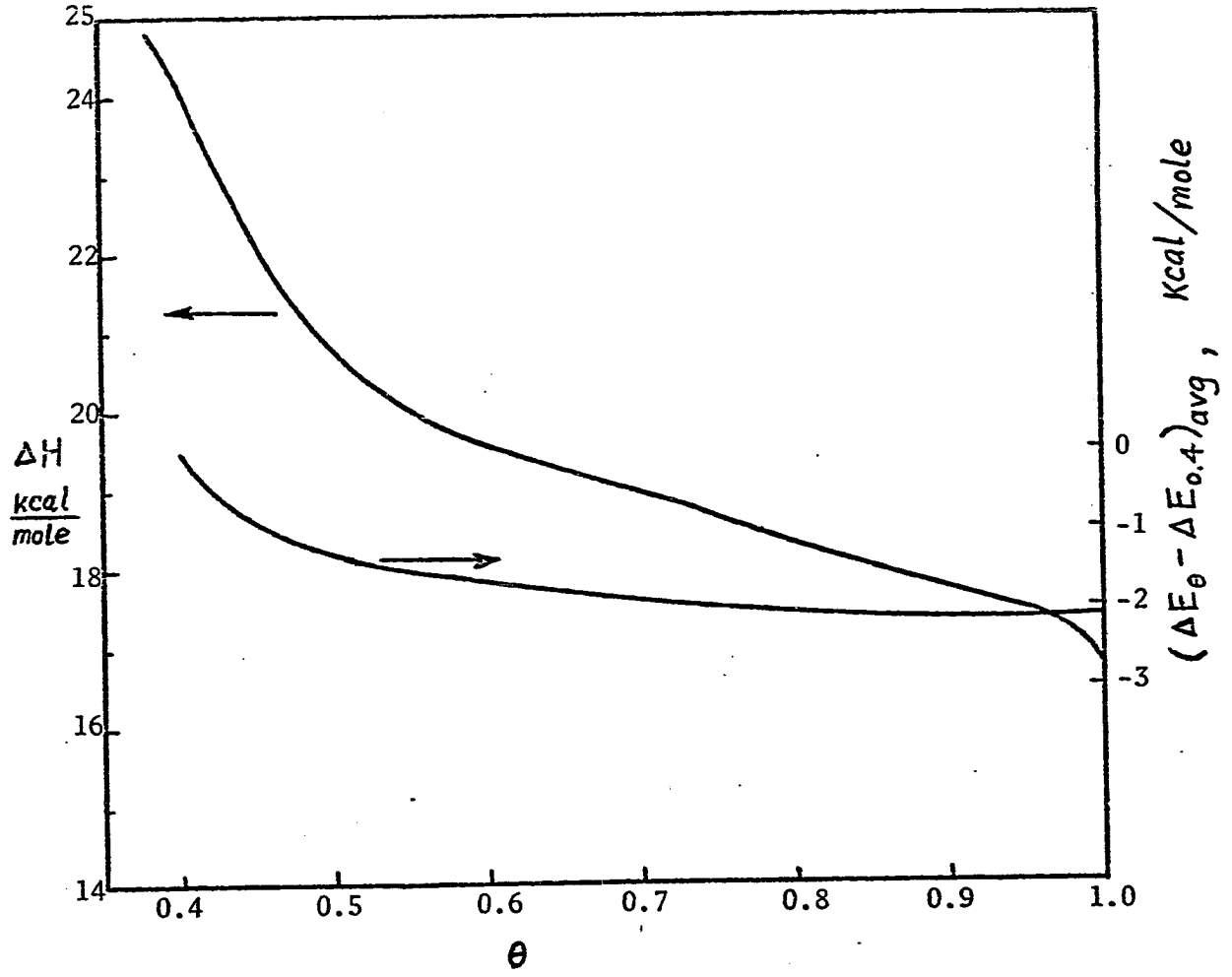

FIG 14

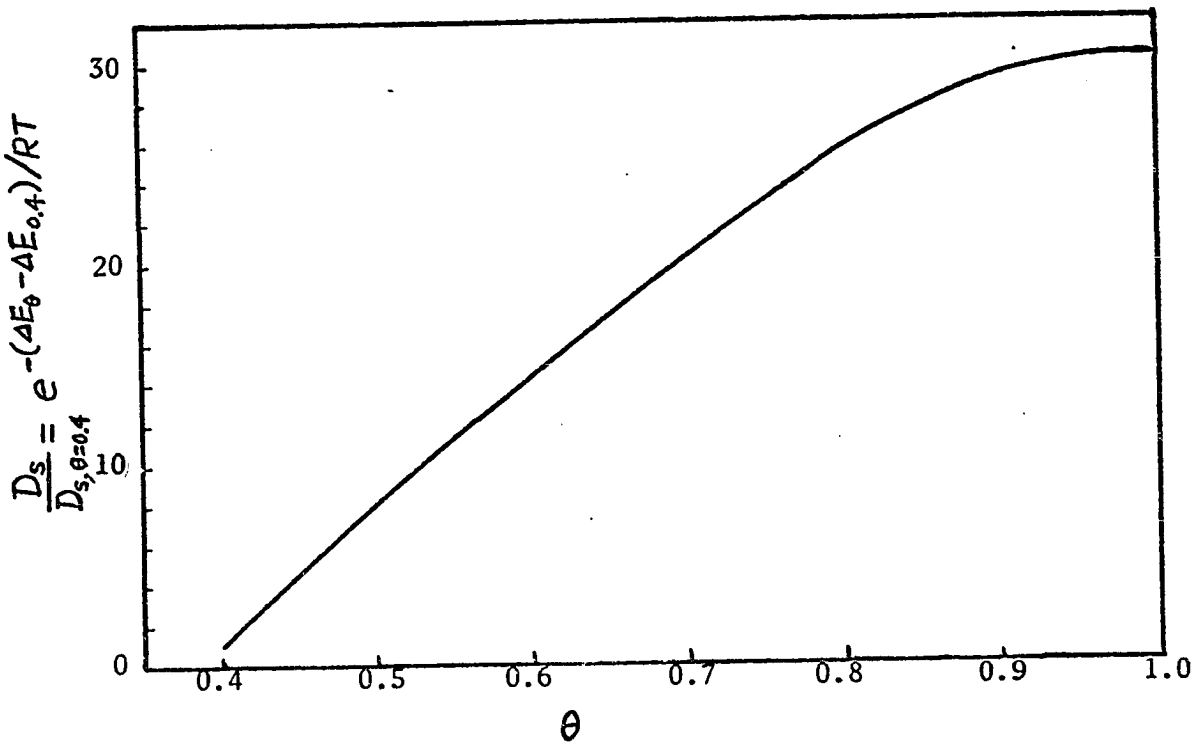

FIG 15

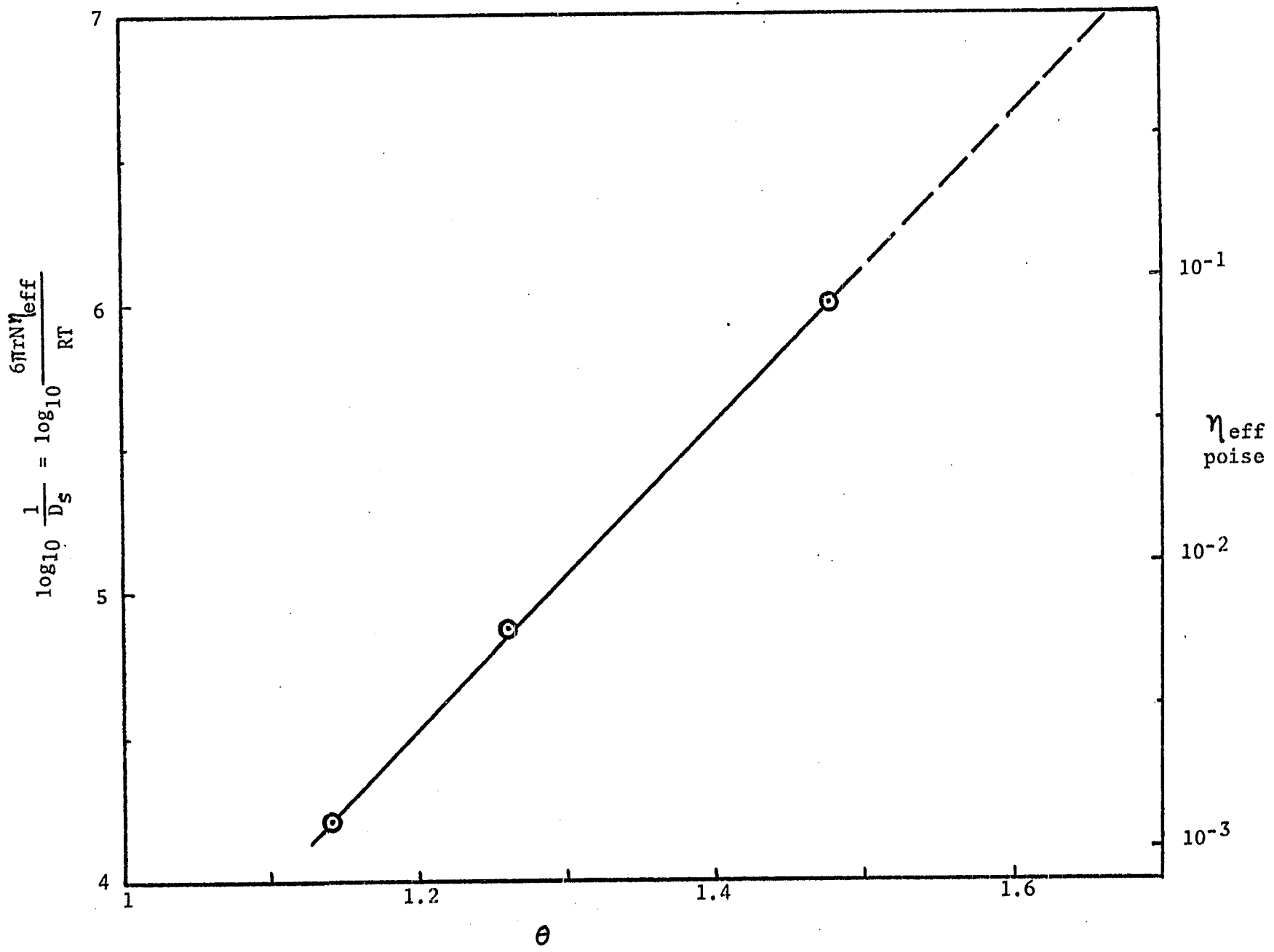

FIG 16

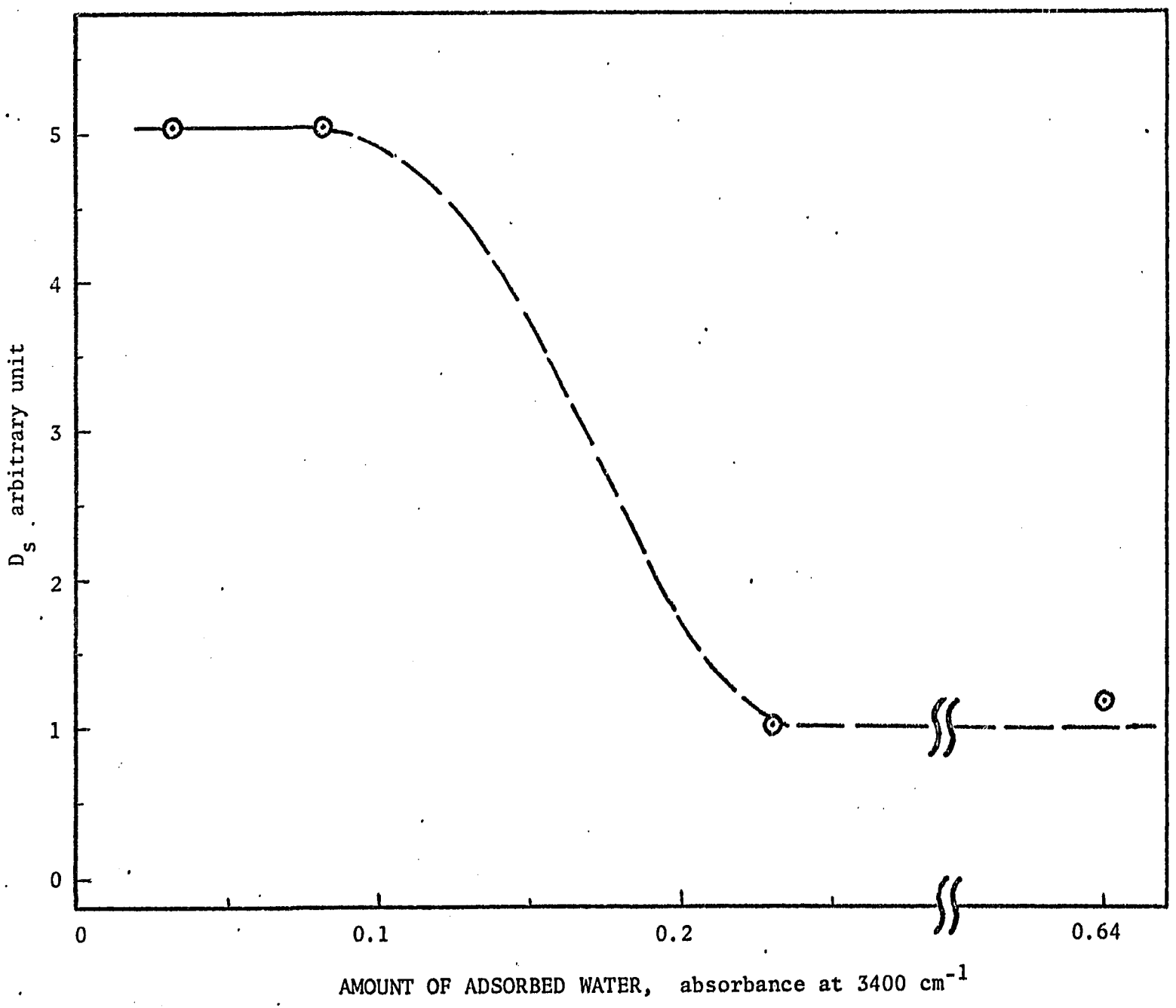

FIG 17

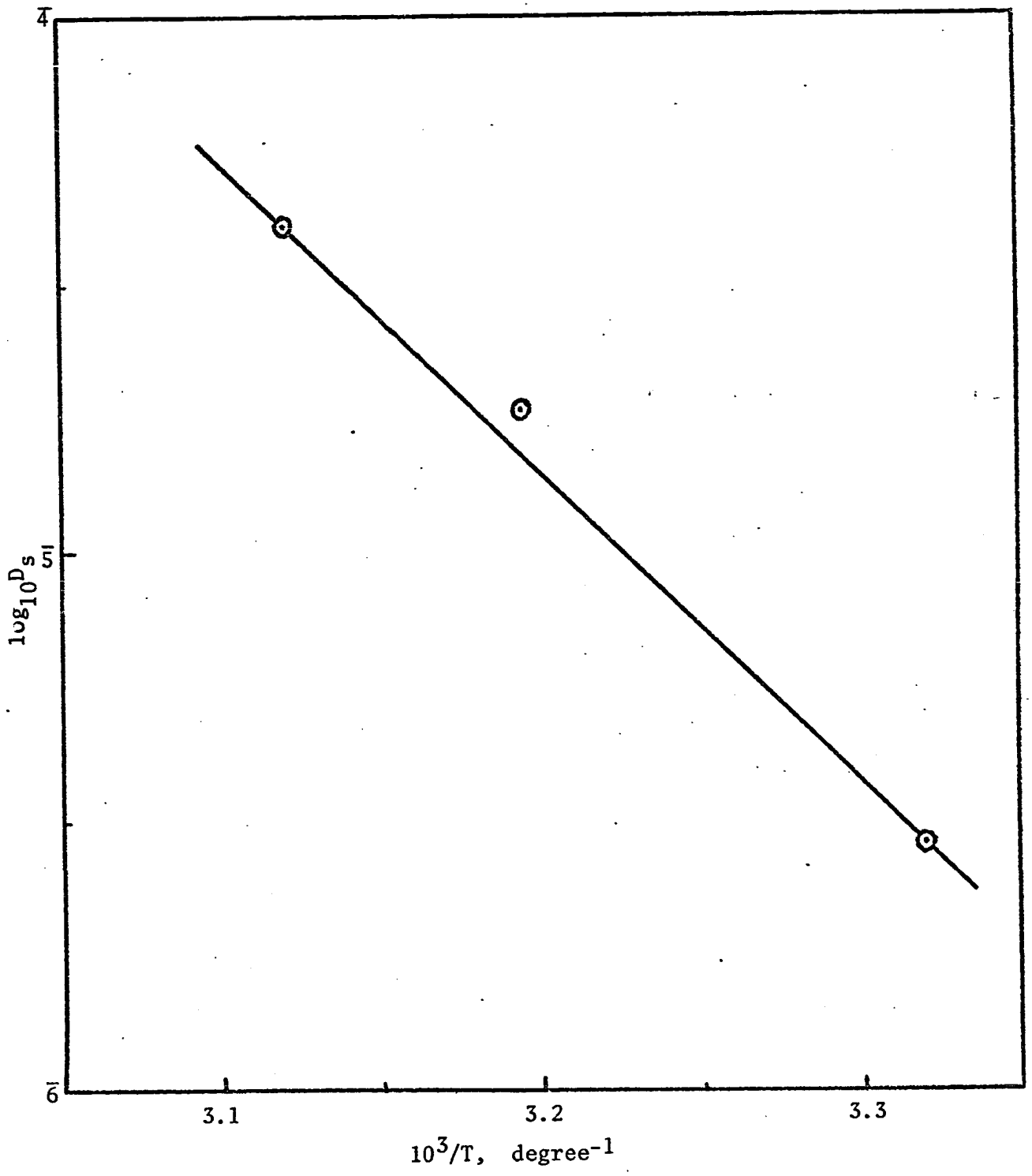

FIG 18 .